

1

1 **Limited effect of the confluence angle and tributary gradient on Alpine confluence**
2 **morphodynamics under intense sediment loads**

3 **Authors:**

4 **Théo St. Pierre Ostrander**⁽¹⁾ – Corresponding Author

5 theo.st-pierre-ostrander@uibk.ac.at

6 **Thomé Kraus**⁽²⁾

7 Thome.Kraus@student.uibk.ac.at

8 **Bruno Mazzorana**⁽³⁾

9 bruno.mazzorana@uach.cl

10 **Johannes Holzner**⁽⁴⁾

11 Johannes.Holzner@provinz.bz.it

12 **Andrea Andreoli**⁽⁵⁾

13 Andrea.Andreoli@unibz.it

14 **Francesco Comiti**⁽⁶⁾

15 Francesco.Comiti@unibz.it

16 **Bernhard Gems**⁽⁷⁾

17 bernhard.gems@uibk.ac.at

18 ^(1, 2, 7) University of Innsbruck, Unit of Hydraulic Engineering, Technikerstraße 13a, 6020, Innsbruck, Austria

19 ⁽³⁾ Universidad Austral de Chile, Faculty of Sciences, Instituto de Ciencias de la Tierra, Edificio Emilio Pugín,
20 Avenida Eduardo Morales Miranda, Campus Isla Teja, Valdivia, Chile

21 ^(4, 5, 6) Free University of Bozen-Bolzano, Faculty of Agricultural, Environmental and Food Sciences,
22 Universitätsplatz 5 - piazza Università, 5, 39100, Bozen-Bolzano, Italy

Formatted: Font: Not Bold

23 **Abstract**

24

25 Confluences are dynamic morphological nodes in all river networks. In mountain regions, they are
26 influenced by hydraulic and sedimentary processes occurring in steep channels during extreme events in
27 small watersheds. Sediment transport in the tributary channel and aggradation in the confluence can be
28 massive, potentially causing overbank flooding and sedimentation into adjacent settlement areas. Previous
29 works dealing with confluences have been mainly focused on lowland regions, or if focused on mountain
30 areas, the sediment concentrations and channel gradients were largely under-representative of mountain
31 river conditions. The presented work contributes to filling this research gap with 45 experiments using a
32 large-scale physical model. Geometric model parameters, applied grain size distribution, and the
33 considered discharges represent the conditions at 135 confluences in South Tyrol (Italy) and Tyrol (Austria).

34 The experimental program allowed for a comprehensive analysis of the effects of (i) the confluence angle,
35 (ii) the tributary gradient, (iii) the channel discharges, and (iv) the tributary sediment concentration. Results
36 indicate, in contrast to most research dealing with confluences, that in the presence of intense tributary
37 sediment supply and a small tributary to main channel discharge ratio (0.1), the confluence angle does not
38 have a decisive effect on confluence morphology. Adjustments to the tributary channel gradient yielded the
39 same results. A reoccurring range of depositional geomorphic units was observed where a deposition cone
40 transitioned to a bank-attached bar. The confluence morphology and tributary channel gradient rapidly
41 adjusted, tending towards an equilibrium state to accommodate both water discharges and the sediment
42 load from the tributary. Statistical analyses demonstrated that confluence morphology was controlled by the
43 combined channel discharge and the depositional or erosional extents by the sediment concentration.
44 Applying the conclusions drawn from lowland confluence dynamics could misrepresent depositional and
45 erosional patterns and the related flood hazard at mountain river confluences.

46

47 **Keywords:** Confluence Morphology; Fluvial Hazard; Steep Tributary; Bedload; Physical Scale
48 Model; Mountain Rivers

49 1 Introduction

50

51 River confluences are important features of all river systems and are sites of significant hydraulic and
52 morphological change (Benda et al., 2004). They are characterized by converging flow paths that produce
53 complex 3-dimensional hydraulics that influence the local morphology, and fluvial dynamics (Best, 1987;
54 1988; Rhoads & Kenworthy, 1995; Benda et al., 2004; Boyer et al., 2006; Ferguson & Hoey, 2008; Guillén-
55 Ludeña et al., 2015; Guillén-Ludeña et al., 2017). In developed areas, confluences form critical junctions as
56 the hydraulic geometries and sediment loads from each channel must be accommodated to avoid overbank
57 flooding and sedimentation (Gems et al., 2014; Liu et al., 2015; Kammerlander et al., 2016; Sturm et al.,
58 2018). The importance of these junctions has garnered much research interest, which has illuminated many
59 characteristics of the hydro-morphodynamic interactions, and the major controls on the flow structure
60 occurring at lowland river confluences (Mosley, 1976; Best, 1987; 1988; Biron et al., 1993; Rhoads &
61 Kenworthy, 1995; Bradbrook et al., 1998; De Serres et al., 1999; Benda et al., 2004; Boyer et al., 2006;
62 Wang et al., 2007; Liu et al., 2015). Best (1987; 1988) built upon the seminal work of Mosley (1976) in his
63 identification of hydraulic and morphologic zones occurring at confluences. The typically occurring hydraulic
64 zones are: flow separation, flow stagnation, flow deflection, maximum velocity, shear layers, and the
65 recovery zone. These zones influence sediment transport pathways through the confluence and the
66 resulting morphological elements of confluences: avalanche faces at the mouth of each confluent channel,
67 a deep central scour hole, and a bar in the separation zone. Best (1988) concluded that the controlling
68 variables as to the location, orientation, and size of these morphologic zones are the confluence angle and
69 the discharge ratio $Q_r = Q_t/Q_m$ which is the ratio of the tributary (Q_t) and the main channel (Q_m) discharges.
70 For lowland confluences increasing the discharge ratio or the confluence angle leads to a greater mutual
71 deflection of flows and a bigger separation zone, which is the largest sink for tributary-transported sediment
72 (Best, 1987, 1988). Flow deflection influences the shear layers generated between the two convergent
73 flows, along which powerful vortices are generated which are responsible for increased bed shear stresses
74 in the junction (Mosley, 1976; Best, 1987; Penna et al., 2018; De Serres et al., 1999). Contrarily, decreasing
75 the confluence angle results in a greater mixing of flows, a smaller separation zone, and declined levels of
76 turbulence in the confluence (Best, 1988; Penna et al., 2018). However, mountain channels are steeper
77 than lowland channels with higher velocities and supercritical flows that amplify event intensity (Rudolf-

78 Miklau et al., 2013) and can result in rapid channel adjustments (Wohl, 2010). This is apparent when
 79 comparing, for example, the Froude numbers from Best (1988) (0.1-1) and Biron et al. (1996) (0.1-0.24),
 80 and the tributary velocities (0.45 m s⁻¹-0.57 m s⁻¹) from Roy and Bergeron (1990) with the Froude numbers
 81 and velocities from the presented work (Table 1) and steep channels in the study region (e.g., Hübl et al.,
 82 2005).

83

84 **Table 1** Experimental discharges for the main (Q_m) and tributary (Q_t) channels with corresponding hydraulic
 85 attributes showing flow depth (h), Froude (Fr), and velocity (v) upstream (u) and downstream (d) of the
 86 confluence and in the tributary channel (t), for all confluence angles (CA) and tributary gradients (trib.).
 87 values are based on undisturbed, initial conditions in the channel.

| | Q_m | Q_t | Q_{tot} | h_u | h_t | h_d | Fr_u | Fr_t | Fr_d | v_u | v_t | v_d |
|--|----------------------|----------------------|----------------------|-------|-------|-------|--------|--------|--------|----------------------|----------------------|----------------------|
| | [l s ⁻¹] | [l s ⁻¹] | [l s ⁻¹] | [m] | [m] | [m] | [-] | [-] | [-] | [m s ⁻¹] | [m s ⁻¹] | [m s ⁻¹] |
| CA 90° Trib. 10% [EXP 1-15] | 15 | 1.5 | 16.5 | 0.04 | 0.01 | 0.03 | 0.58 | 2.04 | 0.77 | 0.35 | 0.68 | 0.44 |
| | 45 | 4.5 | 49.5 | 0.08 | 0.02 | 0.06 | 0.53 | 2.39 | 0.98 | 0.47 | 1.08 | 0.75 |
| | 75 | 7.5 | 82.5 | 0.11 | 0.03 | 0.08 | 0.59 | 2.79 | 1.00 | 0.61 | 1.43 | 0.89 |
| | 105 | 10.5 | 115.5 | 0.14 | 0.04 | 0.10 | 0.62 | 2.63 | 1.01 | 0.73 | 1.52 | 1.01 |
| | 135 | 13.5 | 148.5 | 0.17 | 0.04 | 0.12 | 0.66 | 2.87 | 1.06 | 0.84 | 1.76 | 1.16 |
| CA 90° Trib. 5% [EXP 16-30] | 15 | 1.5 | 16.5 | 0.05 | 0.01 | 0.04 | 0.46 | 1.55 | 0.69 | 0.31 | 0.57 | 0.42 |
| | 45 | 4.5 | 49.5 | 0.09 | 0.03 | 0.07 | 0.50 | 1.79 | 0.80 | 0.47 | 0.90 | 0.71 |
| | 75 | 7.5 | 82.5 | 0.12 | 0.04 | 0.09 | 0.51 | 1.84 | 1.02 | 0.56 | 1.08 | 0.93 |
| | 105 | 10.5 | 115.5 | 0.15 | 0.04 | 0.11 | 0.52 | 1.82 | 1.04 | 0.63 | 1.19 | 1.04 |
| | 135 | 13.5 | 148.5 | 0.18 | 0.05 | 0.13 | 0.52 | 1.90 | 0.97 | 0.69 | 1.34 | 1.08 |
| CA 45° Trib. 10% [EXP 31-45] | 15 | 1.5 | 16.5 | 0.04 | 0.01 | 0.038 | 0.56 | 1.79 | 0.69 | 0.35 | 0.60 | 0.42 |
| | 45 | 4.5 | 49.5 | 0.08 | 0.02 | 0.07 | 0.68 | 2.24 | 0.71 | 0.58 | 1.04 | 0.70 |
| | 75 | 7.5 | 82.5 | 0.11 | 0.03 | 0.09 | 0.61 | 2.54 | 0.96 | 0.64 | 1.34 | 0.89 |
| | 105 | 10.5 | 115.5 | 0.14 | 0.04 | 0.11 | 0.60 | 2.52 | 0.90 | 0.70 | 1.48 | 0.94 |
| | 135 | 13.5 | 148.5 | 0.16 | 0.04 | 0.13 | 0.61 | 2.77 | 0.95 | 0.77 | 1.72 | 1.07 |

Formatted Table

Formatted: Font: Bold

88

89 Confluences in mountain regions have not received the same attention as those in lowland areas, which is
 90 surprising given the hazard potential associated with large volumes of coarse sediment entering these
 91 critical junctions (Aulitzky, 1989). Differentiation between mountain and lowland confluences can be
 92 described by (i) supercritical or transitioning flow conditions in the tributary channel, (ii) bed surface armoring
 93 due to the size heterogeneity of the tributary sediment load or non-erodible conditions in the tributary
 94 channel as a result of hazard protection measures, (iii) high sediment concentrations during flooding events
 95 and (iv) highly variable discharges and sediment transport rates (Aulitzky, 1980; 1989; Meunier, 1991; Roca

96 et al., 2009; Guillén-Ludeña et al., 2017). Topographic confinement can amplify confluence effects, whereas
97 in lowland regions with wide valley floors and broad terraces, deposition cones or fans can be isolated from
98 the main channel (Benda et al., 2004). A sudden introduction of sediment from steep tributaries can trigger
99 numerous types of morphological changes (Benda et al., 2004), as tributaries of confined channel
100 confluences can be particularly disruptive-impactful (Rice, 1998).

101 Detailed records of flash flooding associated with intense sediment transport in Tyrol (Austria) show that
102 these events are a persistent hazard (Embleton-Hamann, 1997; Rom et al., 2023). In the Alps, hazardous
103 events can impact high-population-density valleys. Increased or shifting flooding patterns (Blöschl et al.,
104 2017; Löschner et al., 2017; Blöschl et al., 2020; Hanus et al., 2021) and enhanced sediment availability
105 (Knight & Harrison, 2009; Stoffel et al., 2012; Gems et al., 2020) as a consequence of climate change (Keiler
106 et al., 2010) not only threatens new infrastructure but challenges previously installed mitigation measures.

107 Ancey (2020a) discusses the complications, and assumptions associated with the multitude of approaches
108 used to predict bedload transport and the resulting bedforms, and how rivers are systems punctuated by
109 intense moments of bedload transport resulting in rapid changes in bed morphology over short time intervals
110 (Ancey, 2020b). Relevant hazard events are typically triggered by localized short-duration-high intensity
111 convective storms occurring in small watersheds, which do not significantly affect main channel discharge
112 and bedload transport (Gems et al., 2014; Hübl & Moser, 2006; Prenner et al., 2019; Stoffel, 2010). The
113 narrow, steep tributary provides the sediment load to the main channel, which supplies the dominant flow
114 discharge (Miller, 1958; Guillén-Ludeña et al., 2017).

115 Most of the work that has been done on mountain river confluences has been focused on conditions that
116 do not typically generate hazardous events, mainly under-representations of gradients and sediment
117 concentrations (Roca et al., 2009; Leite Ribeiro et al., 2012a; Leite Ribeiro et al., 2012b; Guillén-Ludeña et
118 al., 2015; Guillén-Ludeña et al., 2017). Complicating the conclusions drawn regarding confluence
119 morphodynamics, St. Pierre Ostrander et al. (2023) established, from a set of 15 experiments, that
120 confluences of mountain rivers are influenced by factors other than the confluence angle and the discharge
121 ratio. They held the confluence angle and discharge ratio constant, only adjusting discharges and tributary
122 sediment concentration. They observed a range of morphologies with specific geomorphic units: a
123 deposition cone, a transitional morphology, a bank-attached bar, and a scour hole. They used unit stream

124 power to predict and associate confluence zone morphology with hydraulic conditions. However, they were
125 limited in their conclusions and recommended further experiments considering additional geometries as
126 their experimental program was not sufficiently comprehensive, restricting the reach of their findings. The
127 channel geometry was unchanged throughout the experimental program, and morphological assessment
128 lacked statistical evaluation and grain size analysis. This paper builds upon these experimental results with
129 an additional 30 experiments considering geometric modifications. In addition to investigating the effects of
130 the channel discharge and sediment concentration, adjustments to the confluence angle and the tributary
131 gradient provide a more comprehensive data analysis of fluvial hazard processes and the resulting
132 morphologies of mountain river confluences. Evaluating morphological patterns and extents was done
133 qualitatively with DEMs of Difference (DoD) created from laser scans, quantitatively from the extents of
134 geomorphic units, depositional and erosional values, and volumetric grain samples, and statistically.
135 Statistical ~~analysis~~ analyses determined which of the ~~introduced factor~~ introduced controlling factors
136 significantly impacted the response variables that define ~~controlling~~ the morphodynamic development of
137 mountain river confluences. Results from the 45 experiments tested the following hypotheses:

- 138 1. Adjustments to the confluence angle and the tributary gradient do not significantly impact
139 confluence morphology and the development of specific geomorphic units (hypothesis 1).
- 140 2. Of the ~~introduced factor~~ introduced controlling factors, the sediment concentration and channel
141 discharge exert the most control over depositional and erosional patterns (hypothesis 2).

142 The formulation of the two hypotheses was based on the results of St. Pierre Ostrander et al. (2023) where
143 it was established that in addition to the confluence angle and discharge ratio, there were additional factors
144 influencing the morphological development of the confluence, and from a review of literature dealing with
145 rivers in response to intense hydrological events. Specifically, a channel will adjust its geometric
146 characteristics and gradient in a way that maximizes sediment transport capacity (Lane, 1955; White et al.,
147 1982).

Formatted: Not Highlight

148

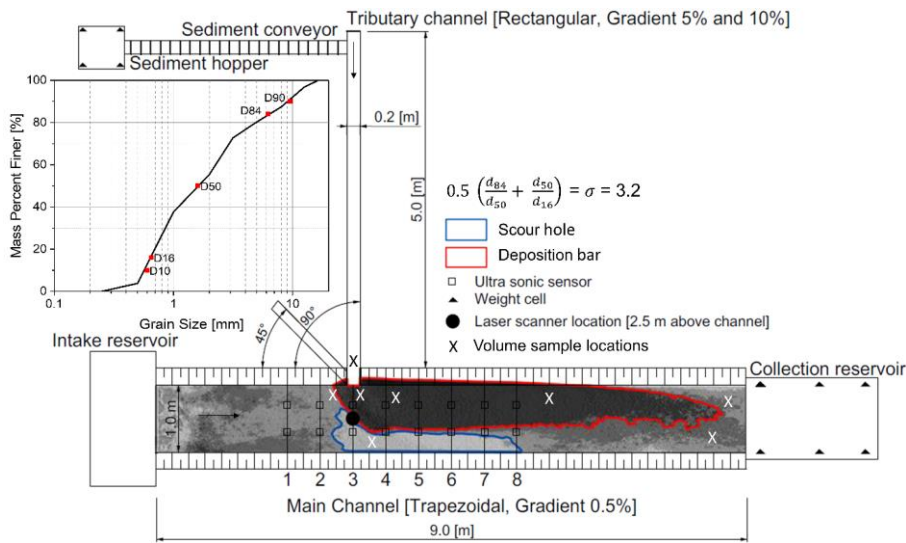
149 2 Model and Methods

150 2.1 Experimental program

151

152 The physical scale model (Fig. 1) was constructed to represent a typical confluence in the regions of South
153 Tyrol (Italy) and Tyrol (Austria). The experimental setup served as a generic configuration to reproduce the
154 main hydrodynamic and sedimentary processes occurring at mountain river confluences while gaining
155 insights into the dominant control variables. Experimental modeling uses and builds upon the configuration,
156 calibration, and experiments (1-15) carried out by St. Pierre Ostrander et al. (2023), ~~but~~ but considers an
157 additional case for the tributary gradient as well as for the confluence angle with an additional tributary
158 gradient and confluence angle. Model dimensions, discharges, and the grain size distribution of the quartz
159 sand input material and the main channel bed were based on an analysis of 135 confluences and 65 volume
160 (subsurface) and line (surface) sediment samples in the study region (St. Pierre Ostrander et al., 2023).
161 The sediment mix was scaled by a factor of 30 to transfer natural grain size dimensions to model conditions.
162 The main channel had a mobile bed, allowing for 0.2_m of erosion ~~and while~~ the tributary channel had a
163 fixed bed. Tributary bed roughness was created using an adhesive to apply a layer of quartz sand to the
164 bed. Channel roughness was established through hydraulic manuals (Chow, 1959) and previous calibration
165 work (St. Pierre Ostrander et al., 2023). Quartz sand is widely used in flume experiments dealing with gravel
166 bed rivers (e.g., Williams, 1970; Gems et al., 2014), as the grain density ($\rho_s=2650 \text{ kg m}^{-3}$) supports Froude
167 model similitude (Young & Warburton, 1996). A grain size distribution curve and the gradation coefficient
168 (σ) of both the mobile bed and the input material are included in Fig. 1. The physical model was adjustable,
169 except for the width of the tributary (0.2-2_m) and the lengths of the channels (5.0-0_m and 9.0_m for the
170 tributary and main channel, respectively). Discharge to each channel was supplied by ~~a~~ separate pumps
171 controlled by ~~an~~ electronic flow measurement devices. The discharge ratio was fixed at 0.1 for all
172 experiments. The tributary sediment discharge was always proportional to the clear water discharge; an
173 increase in tributary discharge meant an increase in both clear water and sediment discharges. The main
174 channel flow was exclusively clear water and fully rough turbulent to replicate typical events that produce
175 massive aggradation at mountain river confluences (Hübl & Moser, 2006; Stoffel, 2010; Gems et al., 2014;

176 Prenner et al., 2019). Scaling was done according to Froude similarity; transferring model dimensions to
 177 nature allows a scale factor range of 20-40. The scale is determined by the width of the tributary at the
 178 confluence relative to the width of the tributary in the physical model and was-is referred to as the specific
 179 scale (St. Pierre Ostrander et al., 2023).



180
 181 **Figure 1** Overview of the physical model showing the location of measurement devices, volume sample
 182 locations, the gradation coefficient (σ), the grain size distribution of the sediment supplied to the tributary
 183 channel and the mobile bed in the main channel, and an example of the scour hole and the deposition bar.

184
 185 Experiments (Table 42) allowed for the same 5 steady-state discharge combinations to be tested with
 186 different tributary gradients, confluence angles, and sediment concentrations, which were based on the bulk
 187 density of the input material. The 5 discharges correspond to flooding conditions in the study region,
 188 including an extreme event. Steady-state discharges were used so a specific discharge could be linked with
 189 a geomorphic unit, to limit uncertainty in associating morphologies with the introduced controlling factors,
 190 which is consistent with other researchers dealing with steep channel confluences, (Roca et al., 2009; Leite
 191 Ribeiro et al., 2012), and to make the morphological development comparable to research dealing with
 192 lowland confluences, which largely assume steady-state conditions (e.g., Mosley, 1976; Best, 1988). The

193 morphological development of the confluence zone for each geometric setup was evaluated by creating
194 DEMs of Difference (DoD) (*ESRI ArcGIS Desktop, Release 10.8.2*) from laser scans (*Faro Focus 3D,*
195 *Trimble X7*) taken before and after an experiment. Each laser scan contained 125 million points with a point
196 density of 0.004 m at a distance of 10 m. The average error between the position of the scanner and the
197 targets used for referencing the scans was less than 0.004 m. The initial bathymetry was the reference,
198 which was established by running a low discharge of 15 l s^{-1} in the main channel for 5 hours to create a
199 more natural river bed, while ~~the~~ post-run bathymetry was the comparison (St. Pierre Ostrander et al.,
200 2023). Morphological evaluation was done by assessing specific zones and overall changes occurring in
201 the channel. The deposition bar and scour hole were delineated by deposition or erosion above or below
202 ~~0.04-01~~ m (Fig. 1). Main channel deposition and erosion areas and volumes reflect morphological change
203 occurring throughout the entire channel above or below the initial bathymetry.

204 Based on ~~historical records~~ incident reports supplied by the Austrian Service for Torrent and Avalanche
205 Control and event documentation (e.g. Hübl et al., 2012), the ~~scaled~~ (30), according to Froude similarity,
206 experiment duration was 20 minutes and started when sediment entered the tributary channel. The only
207 alterations between the experimental groups were changing the tributary gradient and the confluence angle.
208 Experiments 1-15 had a 10-% tributary gradient, a 90° confluence angle, and a main channel gradient of
209 0.5-%. Experiments 16-30 had the same geometric configuration except with a 5-% tributary gradient.
210 Experiments 31-45 had a 10-% tributary gradient and a 45° confluence angle; the main channel gradient
211 remained unchanged. The respective dimensions were chosen as they are the most representative of the
212 study region (St. Pierre Ostrander et al., 2023). DEMs of Difference were created from the DoDs of
213 experiments with identical input conditions, i.e., discharge and sediment supply rate, allowing for a visual
214 assessment of morphological differences based on geometric changes alone. For example, experiments 1
215 and 16 had equal discharges and sediment concentrations; the only change was the tributary gradient, and
216 experiments 1 and 31 had the same discharges, sediment concentrations, and gradients, but the confluence
217 angle was changed. The 10-% gradient tributary with a 90° confluence angle was used as the reference as
218 both geometric configurations are comparable, and changes ~~in~~ from the gradient and confluence angle
219 could be accurately assessed.

Formatted: Not Highlight

Formatted: Font: Not Bold, Not Italic

220 **Table 4-2** Experiment target and actual discharges and sediment concentration, and tributary sediment
 221 supply rate. *Q_t* denotes discharge while *Q_m* or *Q_t* subscripts refer to the main channel and the tributary channel,
 222 respectively. The main channel gradient was 0.5% for all experiments. Experiment 30 was not able to could
 223 not be completed as the deposition in the tributary caused overtopping of the channel.

| EXP | <i>Q_m</i> | | <i>Q_t</i> | | Sed. conc. | | Sed. supply | |
|--|----------------------|----------------------|----------------------|----------------------|------------|--------|-------------------------|-------|
| | Target | Actual | Target | Actual | Target | Actual | rate | |
| [-] | [l s ⁻¹] | [%] | [%] | [kg min ⁻¹] | |
| 10% Tributary Gradient 90° Confluence Angle | 1 | 15.0 | 15.3 | 1.5 | 1.5 | 5.0 | * | 7.6 |
| | 2 | 45.0 | 45.6 | 4.5 | 4.3 | 5.0 | * | 22.9 |
| | 3 | 75.0 | 75.5 | 7.5 | 7.4 | 5.0 | 5.7 | 43.5 |
| | 4 | 105.0 | 104.5 | 10.5 | 10.6 | 5.0 | 4.9 | 53.4 |
| | 5 | 135.0 | 135.4 | 13.5 | 13.4 | 5.0 | 5.2 | 68.7 |
| | 6 | 15.0 | 15.1 | 1.5 | 1.5 | 7.5 | 7.6 | 11.4 |
| | 7 | 45.0 | 46.1 | 4.5 | 4.4 | 7.5 | 7.5 | 34.3 |
| | 8 | 75.0 | 75.3 | 7.5 | 7.5 | 7.5 | 7.3 | 57.2 |
| | 9 | 105.0 | 105.1 | 10.5 | 10.5 | 7.5 | 7.6 | 80.1 |
| | 10 | 135.0 | 134.7 | 13.5 | 13.4 | 7.5 | 7.5 | 103.0 |
| | 11 | 15.0 | 14.8 | 1.5 | 1.5 | 10.0 | * | 15.3 |
| | 12 | 45.0 | 44.9 | 4.5 | 4.6 | 10.0 | 10.1 | 45.8 |
| | 13 | 75.0 | 76.1 | 7.5 | 7.6 | 10.0 | 10.3 | 76.3 |
| | 14 | 105.0 | 105.7 | 10.5 | 10.4 | 10.0 | 10.4 | 106.8 |
| | 15 | 135.0 | 135.4 | 13.5 | 13.6 | 10.0 | * | 137.3 |
| 5% Tributary Gradient 90° Confluence Angle | 16 | 15.0 | 15.9 | 1.5 | 1.4 | 5.0 | * | 7.6 |
| | 17 | 45.0 | 46.0 | 4.5 | 4.5 | 5.0 | 5.1 | 22.9 |
| | 18 | 75.0 | 75.9 | 7.5 | 7.6 | 5.0 | 5.0 | 43.5 |
| | 19 | 105.0 | 104.4 | 10.5 | 10.4 | 5.0 | 5.1 | 53.4 |
| | 20 | 135.0 | 134.7 | 13.5 | 13.5 | 5.0 | 5.2 | 68.7 |
| | 21 | 15.0 | 15.5 | 1.5 | 1.4 | 7.5 | * | 11.4 |
| | 22 | 45.0 | 46.7 | 4.5 | 4.3 | 7.5 | 7.8 | 34.3 |
| | 23 | 75.0 | 74.9 | 7.5 | 7.5 | 7.5 | 7.5 | 57.2 |
| | 24 | 105.0 | 105.5 | 10.5 | 10.4 | 7.5 | 7.5 | 80.1 |
| | 25 | 135.0 | 134.6 | 13.5 | 13.4 | 7.5 | 7.9 | 103.0 |
| | 26 | 15.0 | 15.1 | 1.5 | 1.6 | 10.0 | 9.6 | 15.3 |
| | 27 | 45.0 | 43.5 | 4.5 | 4.4 | 10.0 | 10.2 | 45.8 |
| | 28 | 75.0 | 75.0 | 7.5 | 7.6 | 10.0 | 10.1 | 76.3 |
| | 29 | 105.0 | 105.9 | 10.5 | 10.5 | 10.0 | 10.1 | 106.8 |
| | 30 | 135.0 | - | 13.5 | - | - | - | - |
| 10% Tributary Gradient 45° Confluence Angle | 31 | 15.0 | 14.6 | 1.5 | 1.6 | 5.0 | * | 7.6 |
| | 32 | 45.0 | 45.0 | 4.5 | 4.3 | 5.0 | 5.2 | 22.9 |
| | 33 | 75.0 | 75.8 | 7.5 | 7.7 | 5.0 | 4.9 | 43.5 |
| | 34 | 105.0 | 105.1 | 10.5 | 10.5 | 5.0 | 5.0 | 53.4 |
| | 35 | 135.0 | 134.9 | 13.5 | 13.5 | 5.0 | 5.0 | 68.7 |
| | 36 | 15.0 | 15.0 | 1.5 | 1.5 | 7.5 | * | 11.4 |
| | 37 | 45.0 | 45.6 | 4.5 | 4.5 | 7.5 | 7.6 | 34.3 |
| | 38 | 75.0 | 75.2 | 7.5 | 7.5 | 7.5 | 7.7 | 57.2 |
| | 39 | 105.0 | 106.1 | 10.5 | 10.5 | 7.5 | 7.6 | 80.1 |
| | 40 | 135.0 | 135.6 | 13.5 | 13.4 | 7.5 | 8.0 | 103.0 |
| | 41 | 15.0 | 14.8 | 1.5 | 1.4 | 10.0 | 10.4 | 15.3 |
| | 42 | 45.0 | 44.9 | 4.5 | 4.4 | 10.0 | 10.1 | 45.8 |
| | 43 | 75.0 | 75.5 | 7.5 | 7.6 | 10.0 | 9.9 | 76.3 |
| | 44 | 105.0 | 105.8 | 10.5 | 10.4 | 10.0 | 9.3 | 106.8 |
| | 45 | 135.0 | 135.0 | 13.5 | 13.5 | 10.0 | * | 137.3 |

Formatted: Font: 11 pt, Not Bold, Italic

Formatted: Font: (Default) +Body (Calibri), Italic

Formatted: Font: (Default) +Body (Calibri), Italic

Formatted: Font: +Body (Calibri)

Formatted Table

Formatted: Font: +Body (Calibri)

224 *indicates that the sediment was delivered manually or with manual assistance as the dosing machine could not dose
225 very low or high rates of sediment into the tributary channel

226 2.2 Statistical analysis

227
228 A statistical analysis of the various ~~introduced factor~~introduced controlling factors and their effects on the
229 response variables (Table 23) was done using the software package *OriginPro (v.2023, OriginLab Corp.)*
230 (Stevenson, 2011; Baranovskiy, 2019). The chosen response variables (Table 23), captured either
231 depositional or erosional features; and allowed for a nuanced investigation into the subtle morphological
232 variations that were not able to be qualitatively assessed. The combined discharge was used as a factor
233 since the morphological development of the confluence occurred downstream of the tributary. The
234 confidence interval for all tests was 95-%. A significant result occurred when the p-value, calculated from
235 the test statistic of the applied test, was less than 0.05. A p-value less than 0.05 allowed for rejecting the
236 null hypothesis, which was the factor that did not significantly impact the response variable. If rejected,
237 further pairwise post hoc tests were conducted to determine the decisive factors influencing confluence
238 morphology.

239

240 **Table 2-3 Controlling Factors and response variables that control and define confluence morphology.**

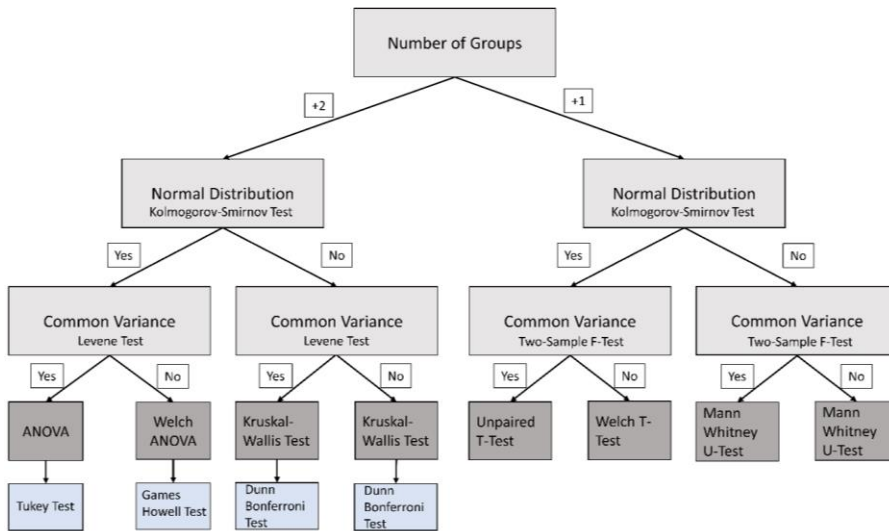
| Factor | Unit | Response Variable | Unit |
|---|-------------------|---|---------------------------------|
| Sediment concentration (5, 7.5, 10) | % | Main channel deposition area and volume | m ² , m ³ |
| Combined discharge (16.5, 49.5, 82.5, 115.5, 148.5) | l s ⁻¹ | Main channel erosion area and volume | m ² , m ³ |
| Confluence angle (90, 45) | ° | Deposition bar area | m ² |
| Tributary gradient (10, 5) | % | Deposition bar length | m |
| | | Deposition bar width | m |
| | | Scour area | m ² |
| | | Scour length | m |
| | | Scour width | m |
| | | Maximum depths scour and deposition | m |

241

242 The sequence of operations in Fig. 2 shows the chosen tests, which allowed for planned comparisons
243 (Ruxton & Beauchamp, 2008). The relevant data sets were examined to ensure that the correct statistical
244 and pairwise post hoc tests were applied (Welch, 1947; Massey, 1951; Dunn, 1964; Maxwell & Delaney,

Formatted Table

245 2004; Steinskog et al., 2007; Sawyer, 2009; McKnight et al., 2010; Moder, 2010; Witte & Witte, 2017;
 246 Delacre et al., 2019). Determining which tests were applied for a specific factor was based on the sample
 247 coming from a population of a specific distribution, then verifying heterogeneity or homogeneity of variances.
 248 This established the following hypothesis and subsequent post hoc tests, if applicable. Not all the tests were
 249 used but were established in case of varying distributions and homogeneity or heterogeneity of variances.
 250 Data was grouped by aggregating individual observations for a specific controlling factor. For example, the
 251 deposition bar area in response to sediment concentration would have 3 groups, a mean area for each of
 252 the 3 tested sediment concentrations; for the confluence angle, the bar area can only have 2 mean values
 253 1 from each angle, so there are only 2 groups.



254
 255 **Figure 2** Workflow for assessing the impacts of controlling factors with associated tests based on the
 256 number of groups, and the distributions and variances of the examined groups data sets.

257

258 **2.3 Volumetric grain sampling**

259

Volume samples were taken after ~~an each~~ experiment with sample locations corresponding to ~~both confluence morphologic (Best, 1988) and hydraulic zones (Best, 1987) in the channel-occurring in the channel.~~ In total 8 samples were taken for each experiment. The sampled volume was 0.002 m^3 with an average sample mass of 3.3 kg which was taken by inserting a cylinder (0.16 m diameter and 0.1 m height) into the channel bed or depositional form. The sampled mass ~~was~~ within the guidelines of Bunte and Abt (2001) (Eq. 42):

$$\text{Mass}_{\text{sample}} (\text{kg}) = 0.1 * 10^b * \rho_s * D_{\text{max}}^3 \quad (\text{Equation 42})$$

Where D_{max} is the maximum grain size (16 mm), ρ_s is grain density (2650 kg m^{-3}), b is the accuracy level, high ($b=5$), medium ($b=4$), low ($b=3$). ~~a~~ larger volume would not be suitable to accurately represent small areas of deposition or erosion as material outside of the area of interest would be additionally captured. The samples were dried after collection and before the sieving analysis. During sieving the material was separated into 10 fractions based on the mesh size of each sieve. The masses of each fraction were determined and plotted as grain size distribution curves. This grain size analysis provided insights into the hydraulic influence on the various zones.

$$\text{Mass}_{\text{sample}} (\text{kg}) = 0.1 * 10^b * \rho_s * D_{\text{max}}^3 \quad (\text{Equation 1})$$

Where D_{max} is the maximum grain size, ρ_s is grain density, b is the accuracy level, high ($b=5$), medium ($b=4$), low ($b=3$)

3 Results

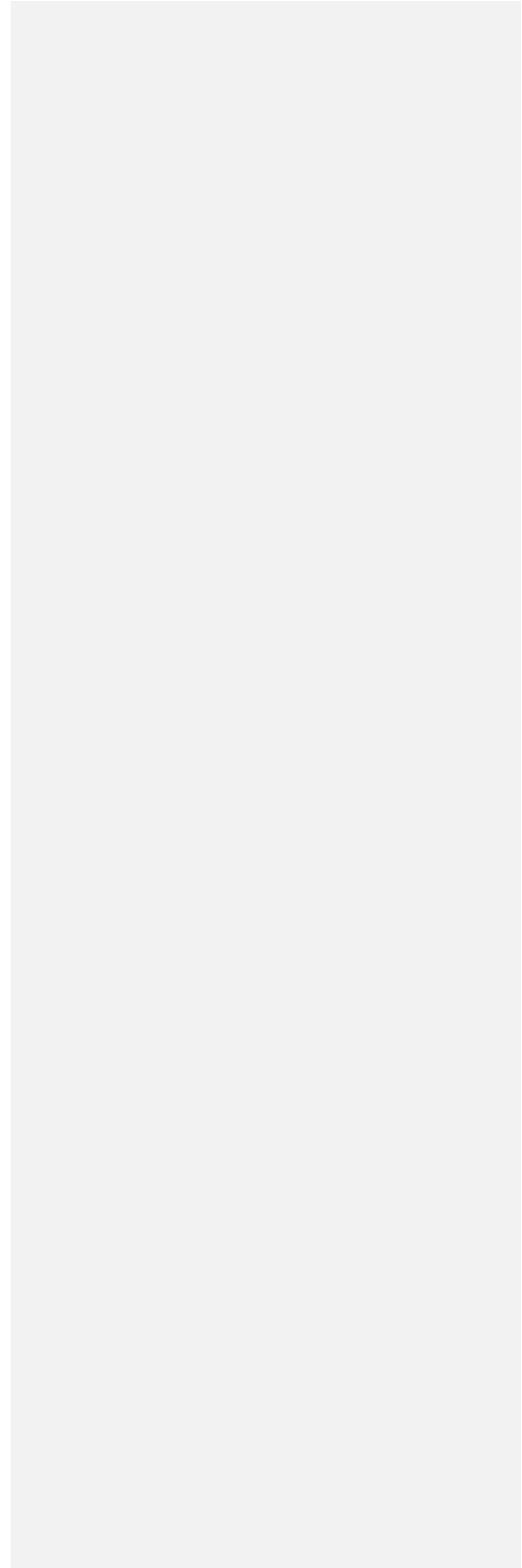
3.1 Development and evolution of confluence morphology

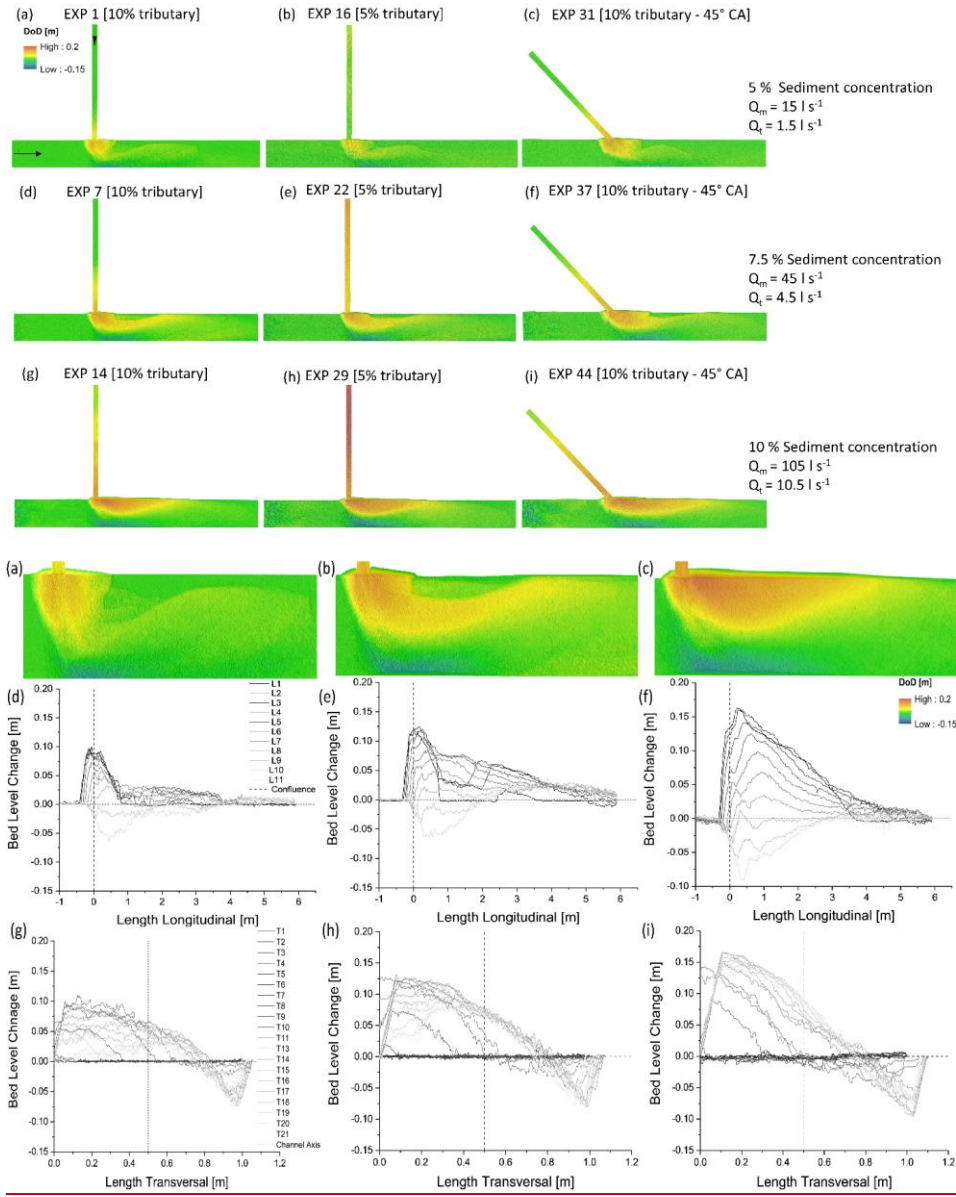
Table ~~3-4~~ associates the three depositional geomorphic units consistently observed for all channel configurations and sediment concentrations with unit stream power. Unit stream power calculations are based on initial conditions at a cross-section in the main and tributary channels. The geomorphic units were (i) the deposition cone (Fig. 3a ~~to 3e~~, Appendix 1a to 9a), (ii) transitional morphology (Fig. ~~3d-3b~~, ~~to~~

Formatted: Justified, Line spacing: Double

Formatted: Not Highlight

322 There was less sediment to be transported and potentially deposited in the scour hole, and the transport
323 capacity of the main channel was not yet exhausted.





324

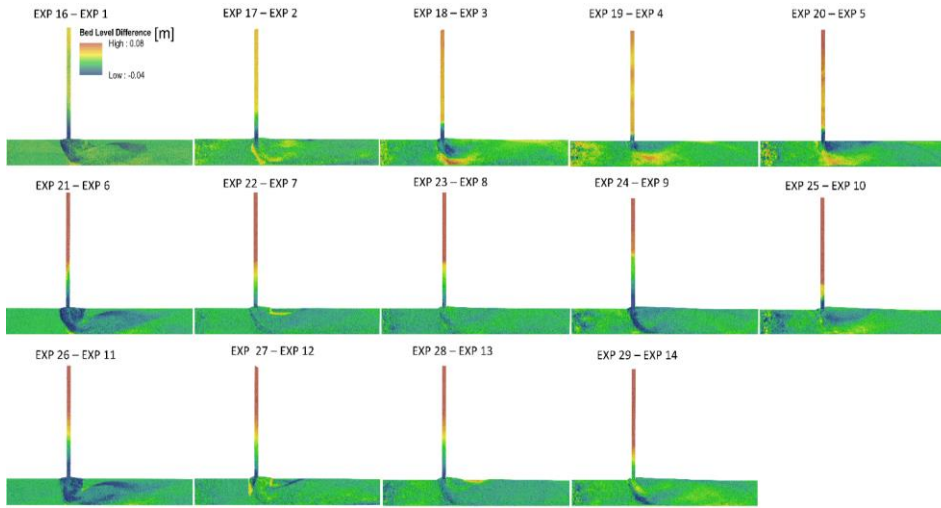
325

326 **Figure 3** Observed geomorphic units, the deposition cone (a) shown with longitudinal (d) and transversal
 327 plots (g), the transitional morphology (d-f) shown with longitudinal (e) and transversal plots (h), and

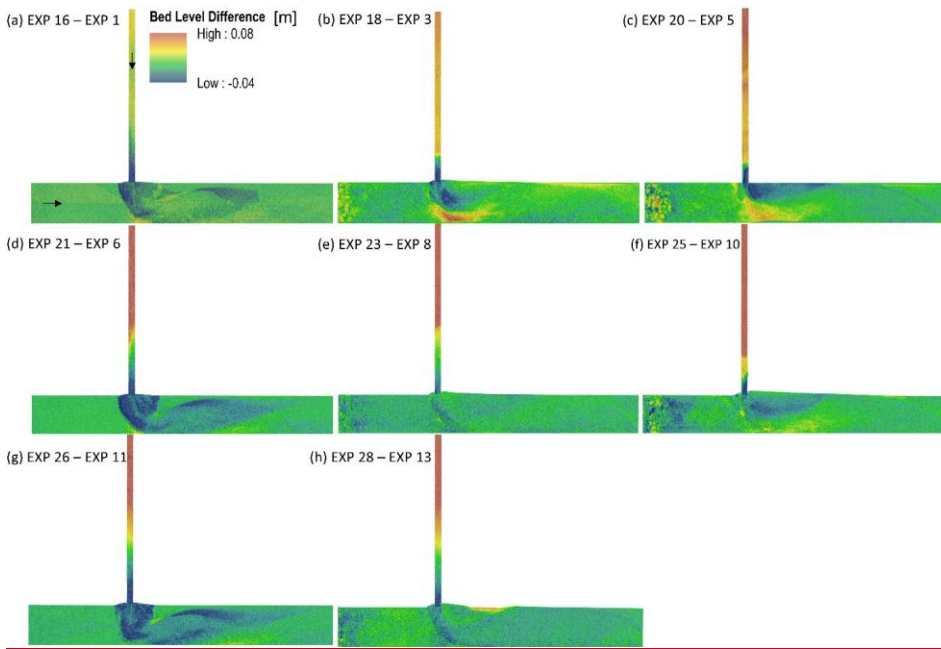
328 ~~the attached-to-channel-wall separation zone bar (g-ci) shown with longitudinal (f) and transversal plots (i)~~
329 ~~geomorphic units~~ with the scour hole on the right, opposite the tributary ~~for all sediment concentrations,~~
330 ~~confluence angles (CA), and tributary gradients.~~ Longitudinal profiles were spaced every 0.1 m and spanned
331 7 m, starting 1 m upstream of the confluence, transversal profiles were spaced every 0.1 m, starting 1 m
332 upstream of the confluence, and spanned 2 m, focusing on the confluence zone.

334 3.2 Effects of the tributary gradient

335
336 Figure 4 shows the DoDs from the minimum (Fig 4a, d, g), median (Fig 4b, e, h), and maximum (Fig 4c, f)
337 experimental discharge combinations which were produced by subtracting the DoDs from experiments 16-
338 30, with a 5-% tributary gradient from experiments 1-15, with a 10-% tributary gradient. The same general
339 morphological patterns consistently occurred regardless of the imposed geometric change. Intense bedload
340 transport in the tributary provided an abundance of sediment to the confluence. A smaller tributary gradient
341 of 5% (EXP 16-30) led to ~~The~~ reduced velocity and subsequent transport capacity which from the decrease
342 ~~in gradient~~ did not greatly impact the morphological development of the confluence, relative to the
343 depositional forms observed when the gradient was 10-% (EXP 1-15). This trend could be associated with
344 the unit stream power of the main channel since the same patterns were observed for all sediment
345 concentrations. As described by Guillén-Ludeña et al. (2017), the main channel supplies the dominant flow
346 at mountain river confluences, if the flow is unchanged then similar development occurs. Main channel unit
347 stream power was consistent for all comparable experiments, the tributary unit stream power was
348 approximately halved when the channel gradient was reduced to 5-% (EXP 16-30) (Table 34).



349



350

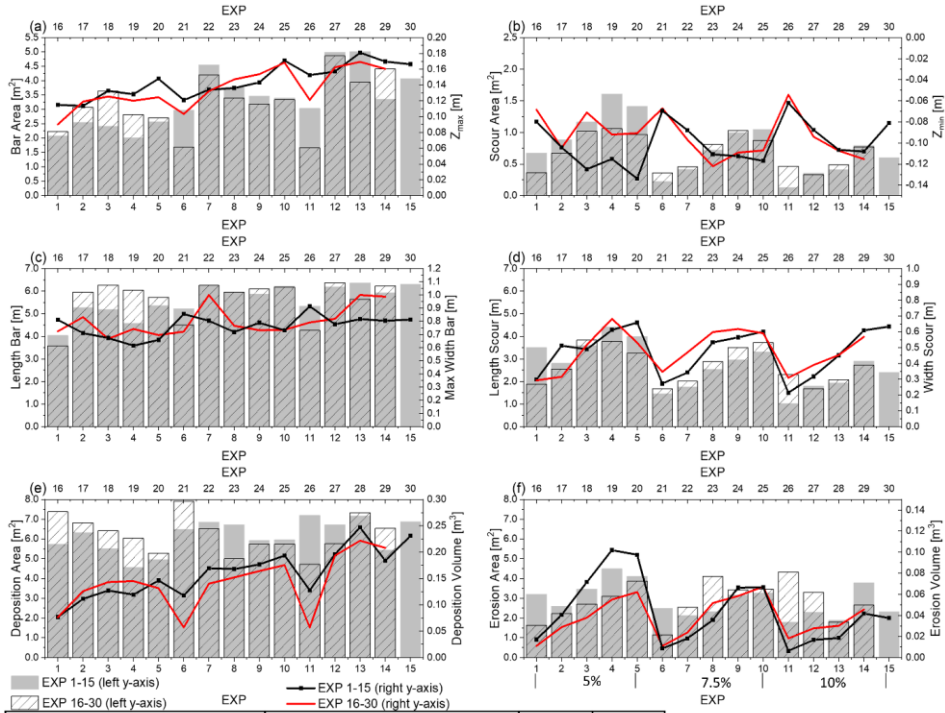
351 **Figure 4** DoDs showing the morphological differences between the minimum (a, d, g), median (b, e, h), and
352 maximum (c, f) experimental discharges which were created by subtracting the DoDs from experiments with

353 a 5-% tributary gradient ([EXP 16-2930](#)) from the DoDs with a 10-% tributary gradient ([EXP 1-4415](#)).
354 ~~supporting a qualitative representation of morphological differences occurring between tributary gradients.~~

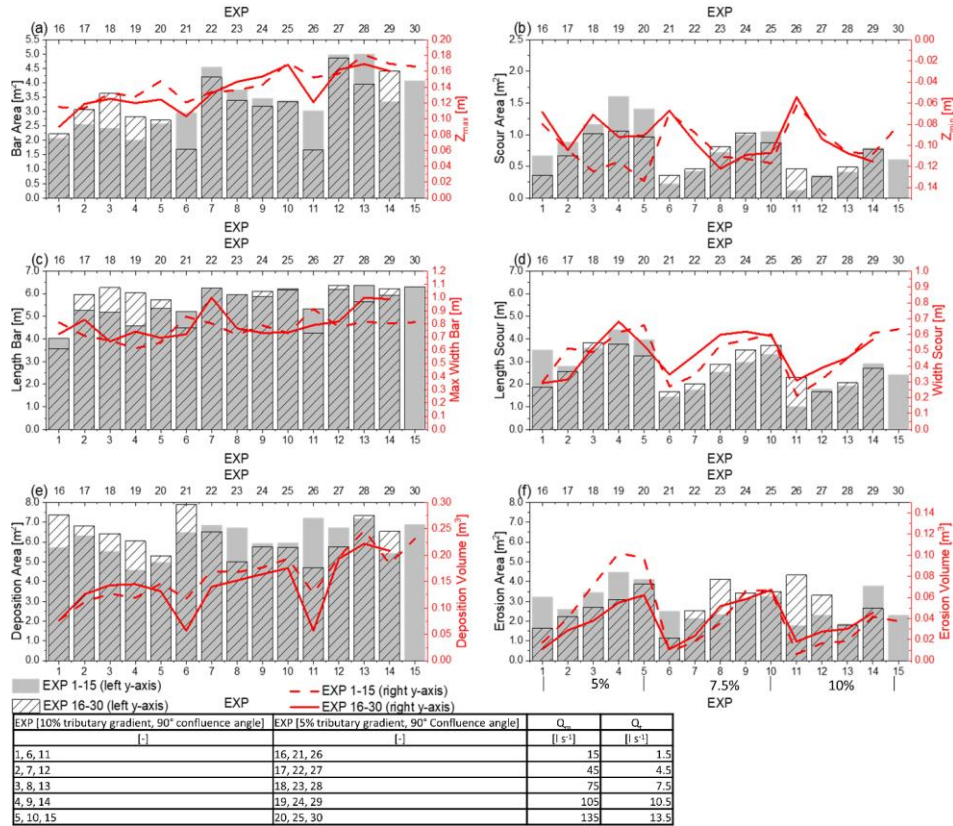
355

356 Figure 5 shows the depositional and erosional characteristics of experiments [1-15 \(10% tributary gradient,](#)
357 [90° confluence angle\)](#) and [16-30 \(5% tributary, 90° confluence angle\)](#) -excluding the tributary channel. A
358 visual inspection of Fig. 5 does not show a clear trend in differences in depositional or erosional
359 characteristics between gradients. What trend could be inferred is most apparent when comparing the first
360 5 experiments for each geometry group ([EXP 1-5 and EXP 16-20](#)). Depositional patterns (Fig. 5a, 5c, and
361 5e) were greater for experiments 16-20 than for experiments 1-5, while erosional patterns were greater for
362 experiments 1-5 than for 16-20 (Fig. 5b, 5d, and 5f). Reducing the tributary channel gradient reduced the
363 velocity of the tributary flow ([Table 1](#)), limiting its contribution to main channel erosion. When the tributary
364 gradient was 10-% ([EXP 1-15](#)), there was greater penetration of the tributary flow into the main channel and
365 a local increase in transport capacity, creating a larger and deeper scour hole and enhanced conveyance
366 of sediment through the confluence.

Formatted: Font color: Text 1



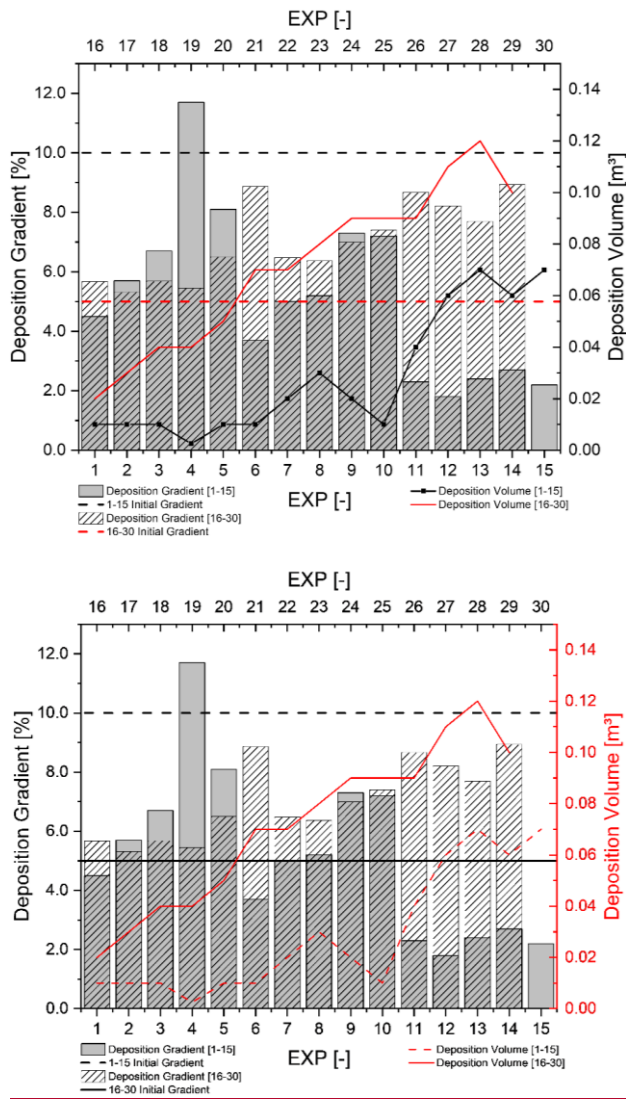
| EXP [10% tributary gradient, 90° confluence angle] | EXP [5% tributary gradient, 90° Confluence angle] | Q_c [l s ⁻¹] | Q_c [l s ⁻¹] |
|--|---|----------------------------|----------------------------|
| 1, 6, 11 | 16, 21, 26 | 15 | 1.5 |
| 2, 7, 12 | 17, 22, 27 | 45 | 4.5 |
| 3, 8, 13 | 18, 23, 28 | 75 | 7.5 |
| 4, 9, 14 | 19, 24, 29 | 105 | 10.5 |
| 5, 10, 15 | 20, 25, 30 | 135 | 13.5 |



368

369 **Figure 5** A comparison of morphological attributes across experiments with a 5-% (EXP 16-30) and 10-%
 370 tributary gradient (EXP 1-15), sediment concentration groups are shown in panel f. Deposition bar and scour
 371 areas (a, b) are delineated by deposition or erosion above or below 0.01_m, respectively. The width and
 372 length values represent the maximum measured width or length (c, d), while the main channel deposition
 373 and erosion areas (e, f) represent all deposition and erosion in the main channel.

374
375
376 Figure 6 shows the gradients and volumes of the deposited sediment in the tributary channel at the end of
377 experiments 1-30. The depositional gradient was determined through a linear regression of the DoD surface
378 profile of the tributary channel relative to the initial tributary channel gradient, and deposition volumes in the
379 tributary channel for experiments 1-30. Adjustments to the tributary gradient changed the depositional
380 mechanisms in the tributary channel, characterized by either an increase or decrease in the gradient of the
381 deposited material in the tributary channel, relative to the initial gradient. When the initial gradient was 10-%
382 (EXP 1-15), the transport capacity of the main channel was the limiting factor for sediment moving through
383 the confluence. This led to a regressive aggradation of sediment, starting at the junction, which decreased
384 the gradient of the tributary channel. Conversely, when the initial tributary channel gradient was 5-% (EXP
385 16-30), the resulting decrease in velocity saturated the transport capacity of the tributary channel.
386 Consequently, the depositional patterns switched, and intense progressive deposition occurred starting at
387 the upstream boundary of the tributary channel which increased the gradient of the channel.



388

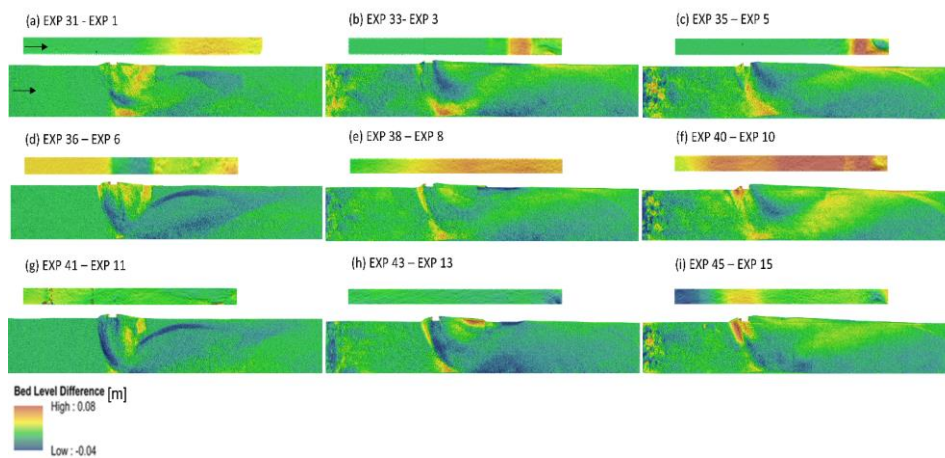
389

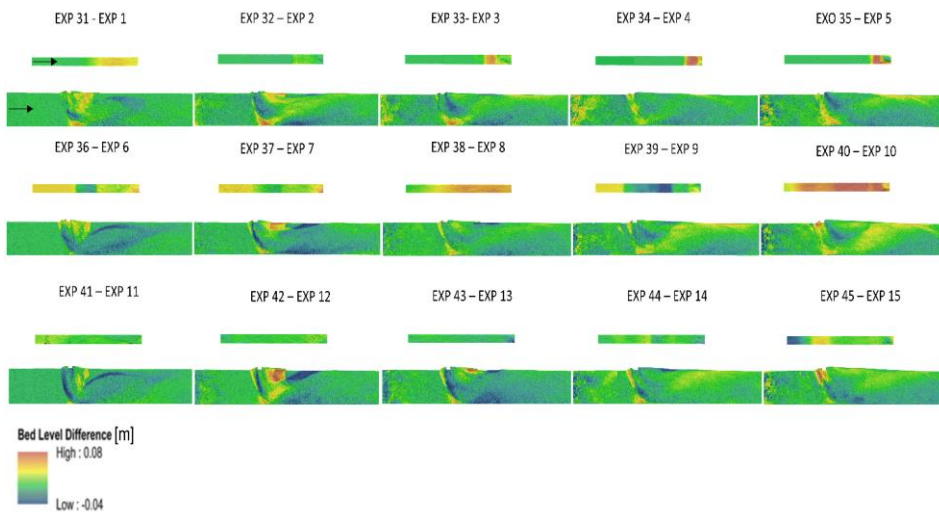
390 **Figure 6** Gradients and volumes of deposited sediment in the tributary channel for experiments 1-15 with
 391 an initial 10% tributary gradient and experiments 16-30 with an initial 5% tributary gradient.

Formatted: Font: 10 pt, Not Italic, Font color: Text 1

3.3 Effects of the confluence angle

Figure 7 shows the DoDs from the minimum (Fig 7a, d, g), median (Fig 7b, e, h), and maximum (Fig 7c, f, i) experimental discharge combinations which were shows the DoD-plots created by subtracting the DoDs produced from experiments with a 45° confluence angle (EXP 31-45) from the DoDs with a 90° confluence angle (EXP 1-15). The tributary channels with a 45° confluence angle were extracted and referenced to the 90° tributary channels allowing for DoD comparisons. A visual inspection of confluence zone morphology does not reveal drastic changes between confluence angle experiments. Small regions of morphological change are apparent, mainly increased deposition downstream of the junction corner and a generally shallower scour hole when the confluence angle was 45°.

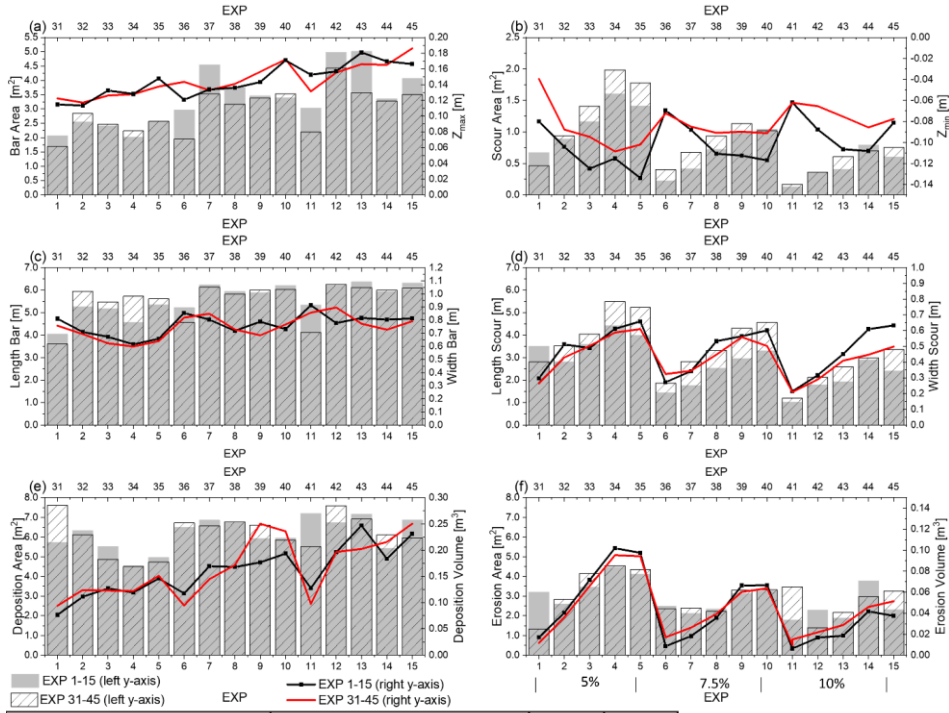




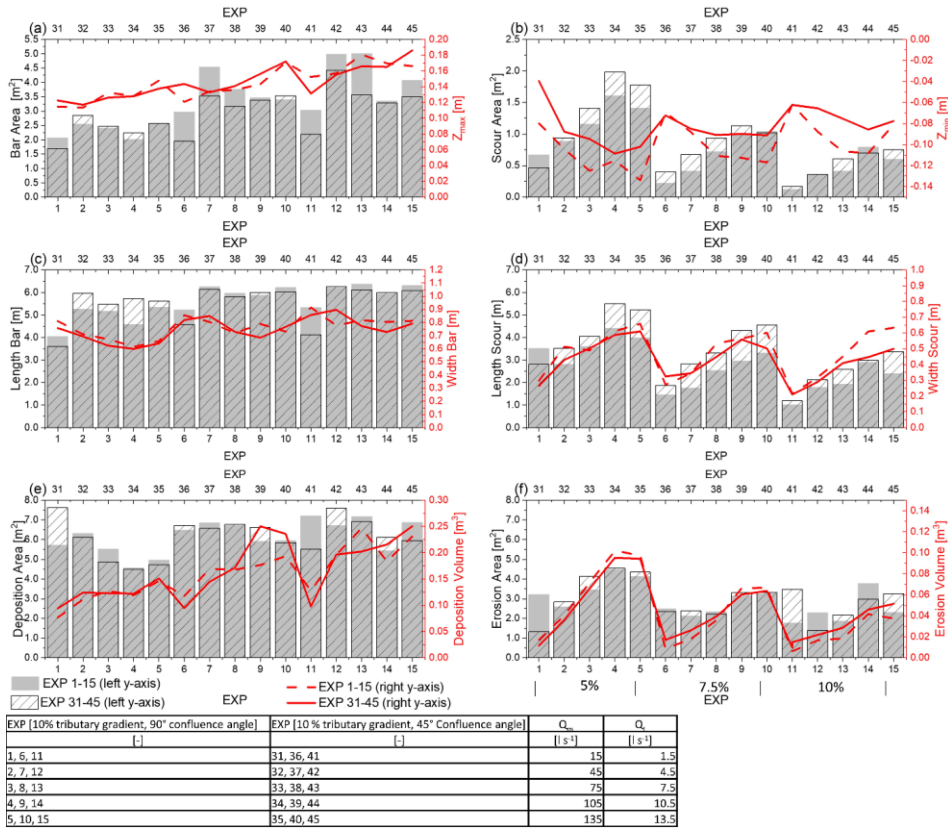
Formatted: Don't keep with next

404
405 **Figure 7** DoDs showing the morphological differences between the minimum (a, d, g), median (b, e, h), and
406 maximum (c, f, i) experimental discharges which were DoDs—created by subtracting the DoDs from
407 experiments with a 45° confluence angle (EXP 31-45) from the DoDs with a 90° confluence angle (EXP 1-
408 15), supporting a qualitative representation of morphological changes occurring between confluence angles.

409
410 Figure 8 shows subtle morphological differences with noticeable trends of scour characteristics, while
411 depositional characteristics do not exhibit standout trends upon visual assessment. Both the length-area
412 and area-length of the scour hole tended to be greater for experiments 31-45, with a 45° confluence angle
413 (Fig. 8b and 8d). However, the depth of scour and width of the scour was generally greater for experiments
414 1-15, with a 90° confluence angle. For both confluence angle experiment groups, a clear trend of increasing
415 scour area, length of scour, and erosion area occurred within each sediment concentration group, increasing
416 in response to discharge. Assessing the impact of confluence angle adjustments on depositional attributes
417 requires-required a statistical approach to reveal any nuanced relationships occurring within the channel.



| EXP [10% tributary gradient, 90° confluence angle] | EXP [10% tributary gradient, 45° Confluence angle] | Q_b [l s ⁻¹] | Q_c [l s ⁻¹] |
|--|--|-------------------------------|-------------------------------|
| 1, 6, 11 | 31, 36, 41 | 15 | 1.5 |
| 2, 7, 12 | 32, 37, 42 | 45 | 4.5 |
| 3, 8, 13 | 33, 38, 43 | 75 | 7.5 |
| 4, 9, 14 | 34, 39, 44 | 105 | 10.5 |
| 5, 10, 15 | 35, 40, 45 | 135 | 13.5 |



419

420

421

422

423

424

425

426

427

428

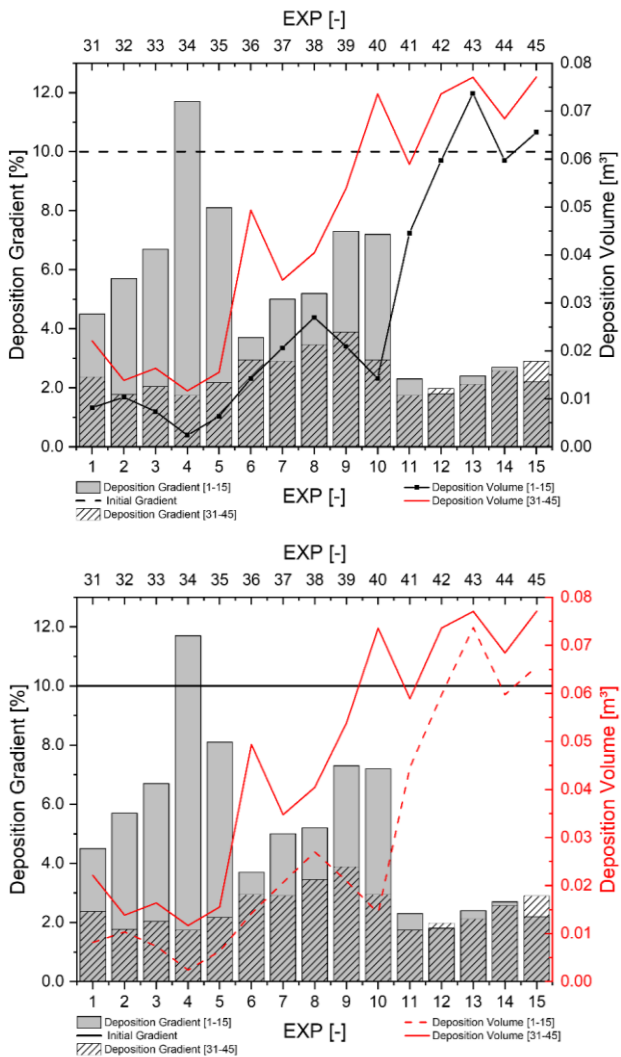
429

Figure 8 Comparison of morphological attributes across experiments with a 45° confluence angle (EXP 31-45) and experiments with a 90° confluence angle (EXP 1-15). Deposition bar and scour areas (a, b) are delineated by deposition or erosion above or below 0.01_m, respectively. The width and length values represent the maximum measured width or length (c, d), while the main channel deposition and erosion areas (e, f) represent all deposition and erosion in the main channel.

Formatted: Don't keep with next

Figure 9 illustrates that variations in tributary depositional properties occurred despite maintaining a consistent tributary gradient across the experimental groups. When the confluence angle was 45° (EXP 31-45), a near overall increase in the depositional volume and a decrease in the depositional gradient was observed (Fig. 9) relative to experiments with a 90° confluence angle (EXP 1-15). A reduction in the

430 confluence angle limits ~~the~~ tributary channel flow penetration into the main channel (Best, 1988), reducing
431 the exposure of the tributary sediment to main channel entraining forces. In the context of experiments 1-
432 15, with a greater confluence angle (90°), the penetration of the tributary channel exhibited a greater extent.
433 Increasing the confluence angle caused a greater mutual deflection of flows, further segregating the
434 tributary and main channel flows (Best, ~~1988~~1987). This factor, coupled with the increased velocity, allowed
435 the tributary sediment load to rapidly pass through the confluence zone when the confluence angle was
436 greater-90° rather than be deposited in the tributary channel.



437

438

439 **Figure 9** Gradients and volumes of deposited sediment in the tributary channel for experiments 1-15 (10%

440 tributary gradient, 90° confluence angle) and 31-45 (10% tributary gradient, 45° confluence angle).

441 **3.4 Statistical evidence analysis of controlling factors impacting confluence morphology**

Formatted: Don't keep with next, Don't keep lines together

442 **3.4.1 Overview**

443
 444 Only controlling factors that had a significant effect-effect (Table 45) on the response variables of the main
 445 channel are discussed. The focus of the statistical analysis is-was to determine the dominant controls over
 446 confluence morphology. For this reason, tributary channel depositional behavior is-was not included as a
 447 response variable.

448
 449 **Table 4-5 Introduced factor, introduced controlling factors** and their impact on confluence morphology, bold
 450 text indicates the factor had a significant impact on one or more groups of the response variable. P-values
 451 from overall mean comparison tests are included.

Formatted: Don't keep with next

| Factor | Z _{max} | Z _{min} | Deposition area | Deposition volume | Erosion area | Erosion volume | Bar area | Bar length | Bar width | Scour area | Scour length | Scour width |
|------------------------|-------------------------------------|------------------|-----------------|-------------------|--------------|----------------|----------|------------|-----------|------------|--------------|-------------|
| Sediment concentration | <.0001 .001 | .30 | .09 | .001 | .19 | .015 | 2.85E-4 | .059 | <.0001 | 4.38E-4 | 3.63E-4 | .30 |
| Discharge | .004 | <.0001 | .047 | <.0001 | .007 | <.0001 | 1.89E-4 | <.0001 | .14 | <.0001 | <.0001 | <.0001 |
| Tributary gradient | .20 | .78 | .82 | .24 | .96 | .50 | .27 | .79 | .21 | .33 | .35 | .55 |
| Confluence angle | .46 | 0.022 | .91 | .40 | 0.84 | .67 | .25 | .81 | .37 | .23 | .047 | .267 |

Formatted Table

452

Formatted: Line spacing: Double

453 **3.4.2 Sediment concentration**

454
 455 Table 5-6 and Fig. 10 show that sediment concentration had a significant impact on 7 out of 12 response
 456 variables. Increased or decreased sediment concentration provoked-enhanced depositional or erosional
 457 patterns, respectively, while decreased sediment concentration enhanced erosional patterns. Post hoc
 458 testing further revealed patterns caused by the sediment concentration (Table 56). Unsurprisingly, the
 459 majority of the significant differences in mean response values occurred between 5-% and 10-% sediment
 460 concentration groups. The maximum deposition depth was significantly reactive to all sediment
 461 concentrations, With increasingas the sediment concentration increased the deposition depth increased,
 462 but reached a maximum as aggradation cannot exceedis regulated by the local flow depth. When the

463 sediment ~~concentration~~concentration was 7.5-%, the response variables did not significantly differ from those
464 of the 5-% and 10-% groups.

465 **Table_56** Sediment concentration and its impact on the response variables; σ is the standard deviation.
 466 ~~Post hoc~~Pairwise post hoc mean comparison testing is summarized with letters A, B, and C. ~~If sediment~~
 467 ~~concentration groups share a letter then there is no significant difference in the pairwise comparisons of~~
 468 ~~means; if the letters are different then a significant difference was detected.~~Means that do not share a letter
 469 are significantly different. For example, the mean Z_{max} for each sediment concentration group was
 470 significantly different (A, B, C), but the mean deposition volume for ~~sediment~~7.5% and ~~10%~~sediment
 471 concentration groups did not significantly differ from each other (B, B) but were significantly different from
 472 the mean deposition volume when the sediment concentration was 5% (A).

Formatted: Don't keep with next

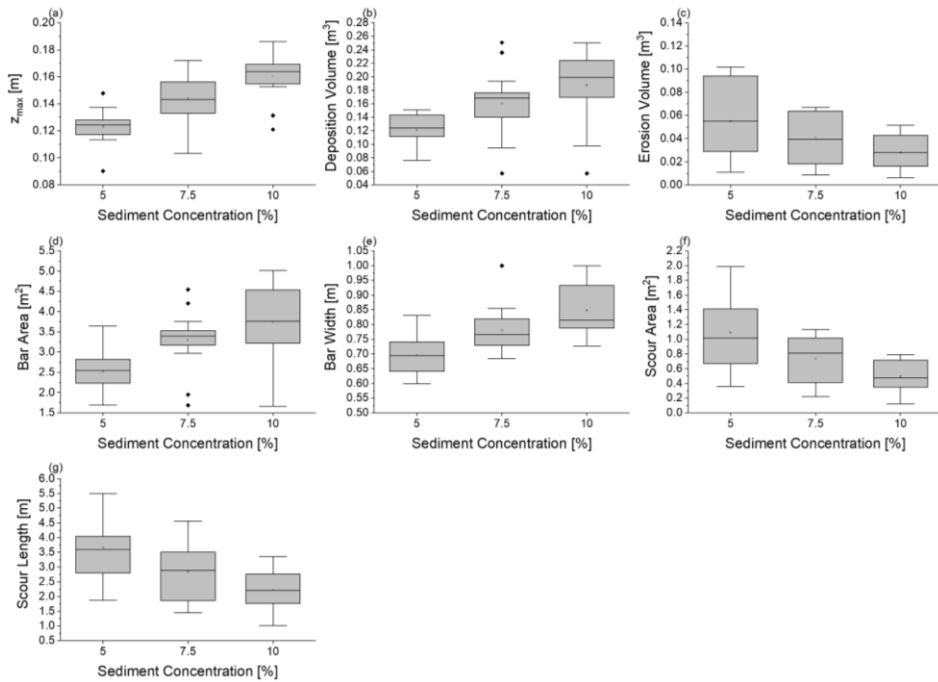
Formatted: Font: Not Italic

Formatted: Font: Not Italic

Formatted: Font: Not Italic

| Response Variable | σ | | | Test | Difference in Means | Post hoc Test | 5 | 7.5 | 10 |
|---------------------------------------|----------|-------|-------|------------------------|---------------------|---------------|-------|-------|-------|
| | 5% | 7.5% | 10% | | | | | | |
| [-] | [-] | [-] | [-] | [-] | [-] | [-] | [%] | [%] | [%] |
| Z_{max} [m] | 0.01 | 0.02 | 0.02 | ANOVA (F = 18.5) | Yes | Tukey-Test | A | B | C |
| Z_{min} [m] | 0.02 | 0.02 | 0.02 | ANOVA (F = 1.2) | No | | | | |
| Deposition area [m ²] | 1.00 | 0.68 | 0.85 | ANOVA (F = 2.4) | No | | | | |
| Deposition volume [m ³] | 0.02 | 0.05 | 0.06 | ANOVA (F = 8.2) | Yes | Tukey-Test | A | B | B |
| Erosion area [m ²] | 1.02 | 0.74 | 0.87 | ANOVA (F = 1.7) | No | | | | |
| Erosion volume [m ³] | 0.03 | 0.02 | 0.01 | Welch ANOVA (F = 4.9) | Yes | Games-Howell | A | A/B | B |
| Deposition bar area [m ²] | 0.47 | 0.72 | 1.01 | Welch ANOVA (F = 11.5) | Yes | Games-Howell | A | B | B |
| Length bar [m] | 0.88 | 0.57 | 0.74 | ANOVA (F = 3.0) | No | | | | |
| Width bar [m] | 0.07 | 0.08 | 0.09 | ANOVA (F = 13.3) | Yes | Tukey-Test | A | B | B |
| Scour area [m ²] | 0.47 | 0.30 | 0.22 | Welch ANOVA (F = 10.6) | Yes | Games-Howell | A | A | B |
| Length scour [m] | 0.96 | 0.96 | 0.67 | ANOVA (F = 9.7) | Yes | Tukey-Test | A | B | B |
| Width scour [m] | 0.14 | 0.12 | 0.14 | ANOVA (F = 1.3) | No | | | | |

473
 474 Adjustments in deposition and erosion areas allowed for the majority of the incoming sediment load to pass
 475 through the confluence. However, given the differences in sediment loads, rapid mutual adjustments were
 476 morphologically represented by the same general patterns but with less erosion and more aggradation as
 477 sediment concentration ~~increases~~increased. The differences in mean response values between the
 478 experiments with 5-% and 10-% tributary sediment concentrations and the similarities to the mean response
 479 values, when the sediment concentration was 7.5-%, can be attributed to this process.



480

481 **Figure 10** Boxplots from ANOVA and Welch ANOVA results for all response variables that showed a
 482 significant difference in mean values [\(Table 5\)](#) with sediment concentration as the [controlling](#) factor.

483

484 3.4.3 Combined discharge

485

486 Table [6-7](#) and Fig. 11 show that the discharge significantly [affected-affected](#) 11 out of 12 response variables.

487 Generally, erosional processes increased with increasing discharge as the transport capacity of the main

488 channel flow increased. At lower discharges with limited transport capacity, erosional processes were

489 comparatively reduced. However, certain instances revealed increased depositional properties with

490 increasing discharge (Fig. 11a and 11d). This most apparently occurred between the 16.5 l s^{-1} and 49.5 l s^{-1}

491 ¹ combined discharge experiments. A deposition cone formed across all sediment concentrations when the

492 combined discharge was 16.5 l s^{-1} . Unlike the bar or transitional morphology, the deposition cone does not

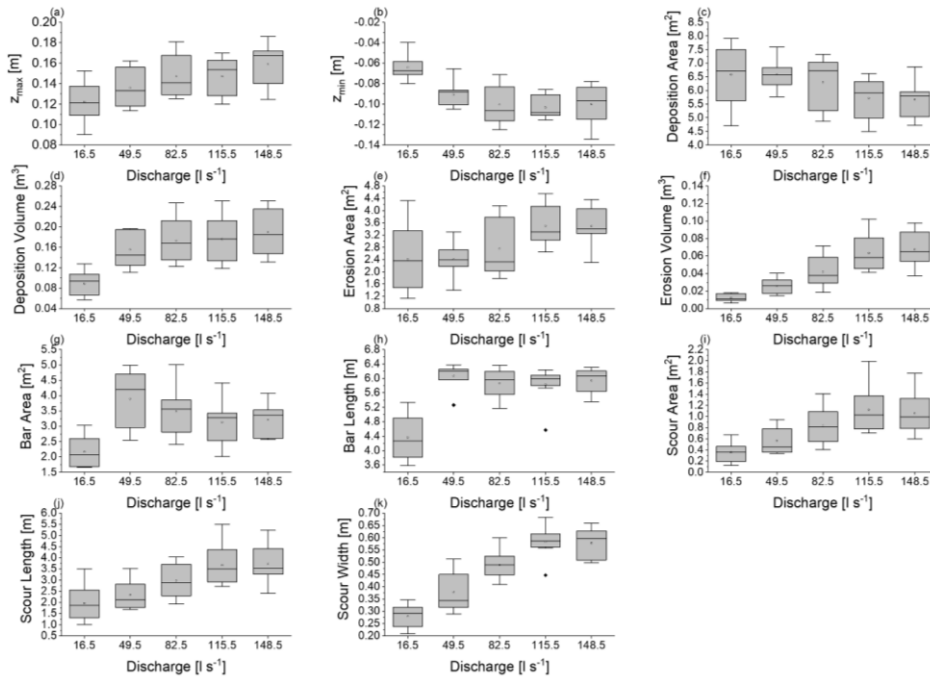
493 occupy the separation zone and is characterized by a short longitudinal extent while protruding furthest into
 494 the main channel from the tributary channel. At discharges at and above 49.5 l s⁻¹, the depositional patterns
 495 shifted, and sediment was entrained and deposited in the separation zone. The separation zone is the
 496 largest sink for tributary-transported sediment; the occupying bar can only be as big as the hydraulic zone,
 497 which is the same size for a given discharge ratio (Best, 1987; 1988). This explains the subtle differences
 498 in depositional properties once the combined discharge exceeded 49.5 l s⁻¹.

499
 500 **Table 6-7** Discharge and its impact on the response variables; (σ) is the standard deviation. Pairwise post
 501 hoc mean comparison testing is summarized with letters A, B, C, and D; means that do not share a letter
 502 are significantly different. Post-hoc testing is summarized with letters A, B, C, and D if discharge groups
 503 share a letter then there is not a significant difference in the pairwise comparisons of means, if the letters
 504 are different then a significant difference was detected.

| Response Variable | σ | | | | | Test | Diff. in means | Post Hoc Test | 16.5 | 49.5 | 82.5 | 116 | 149 |
|----------------------------------|-----------------------|-----------------------|-----------------------|-----------------------|-----------------------|------------------------|----------------|---------------|-----------------------|-----------------------|-----------------------|-----------------------|-----------------------|
| | 16.5 | 49.5 | 82.5 | 115.5 | 148.5 | | | | | | | | |
| [-] | [l s ⁻¹] | [l s ⁻¹] | [l s ⁻¹] | [l s ⁻¹] | [l s ⁻¹] | [-] | [-] | [-] | [l s ⁻¹] | [l s ⁻¹] | [l s ⁻¹] | [l s ⁻¹] | [l s ⁻¹] |
| Z _{max} [m] | 0.02 | 0.02 | 0.02 | 0.02 | 0.02 | ANOVA (F = 4.5) | YES | Tukey-Test | A | A/B | A/B | A/B | B |
| Z _{min} [m] | 0.01 | 0.01 | 0.02 | 0.01 | 0.02 | ANOVA (F = 10.7) | YES | Tukey-Test | A | B | B | B | B |
| Deposition [m ²] | 1.07 | 0.52 | 0.93 | 0.77 | 0.68 | ANOVA (F = 2.7) | YES | Tukey-Test | A | A | A | A | A |
| Deposition [m ³] | 0.02 | 0.03 | 0.04 | 0.04 | 0.05 | ANOVA (F = 9.3) | YES | Tukey Test | A | B | B | B | B |
| Erosion area [m ²] | 1.08 | 0.52 | 0.92 | 0.66 | 0.63 | ANOVA (F = 4.1) | YES | Tukey Test | A | A | A/B | B | A/B |
| Erosion volume [m ³] | 0.004 | 0.01 | 0.02 | 0.02 | 0.02 | Welch ANOVA (F = 28.9) | YES | Games-Howell | A | B | B/C | C | C |
| Bar area [m ²] | 0.52 | 0.91 | 0.79 | 0.71 | 0.54 | ANOVA (F = 7.2) | YES | Tukey Test | A | B | B | B | B |
| Length bar [m] | 0.62 | 0.33 | 0.38 | 0.5 | 0.34 | ANOVA (F = 22.0) | YES | Tukey Test | A | B | B | B | B |
| Width bar [m] | 0.06 | 0.11 | 0.11 | 0.12 | 0.06 | ANOVA (F = 1.9) | NO | | | | | | |
| Scour area [m ²] | 0.17 | 0.24 | 0.33 | 0.42 | 0.38 | ANOVA (F = 9.1) | YES | Tukey Test | A | A/B | B/C | C | C |
| Length scour [m] | 0.8 | 0.63 | 0.76 | 0.92 | 0.87 | ANOVA F = 8.4) | YES | Tukey Test | A | A | A/B | B | B |
| Width scour [m] | 0.05 | 0.08 | 0.06 | 0.06 | 0.06 | ANOVA (F = 36.9) | YES | Tukey Test | A | B | C | D | D |

505
 506 Pair-wise post hoc comparisons of maximum deposition depth indicated a significant difference in mean
 507 values between the lowest and highest combined discharge experiments while revealing similarities among
 508 intermediate discharge scenarios. These similarities could be attributed to the combined flows regulating
 509 the depositional depth, which does not exceed the flow depth. The observed differences can be attributed
 510 to the increased sediment load and associated morphological changes with increasing discharge.

Formatted: Font: (Default) Arial



511
 512 **Figure 11** Boxplots from ANOVA and Welch ANOVA results for all response variables that showed a
 513 significant difference in mean values (Table 5) with combined discharge as the controlling factor.

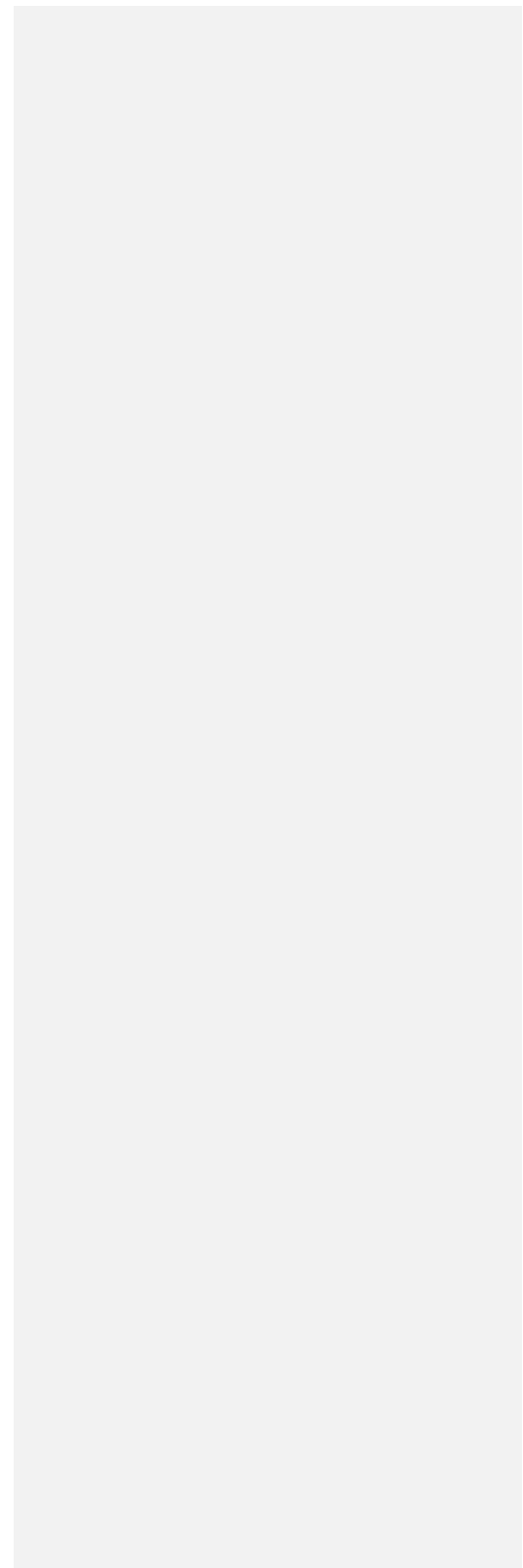
514

515 3.4.4 Confluence angle

516

517 Surprisingly, the confluence angle only had a significant influence on 2 out of the 12 of the response
 518 variables (Table 73). The confluence angle did have a decisive impact on scour depth (Fig. 12a). This could
 519 be attributed to the degree of turbulence increasing with increasing confluence angle which enhanced the
 520 ability of the flow to scour the bed (Mosley, 1976). The elevated turbulence arises from the increased mutual
 521 flow deflection, which influences the shear layers generated between the two converging flows. Along these
 522 shear layers, powerful vortices are created which enhance the bed shear stress within the junction, resulting
 523 in significant bed scour (Best, 1987). Reducing the confluence angle allowed for improved mixing of tributary

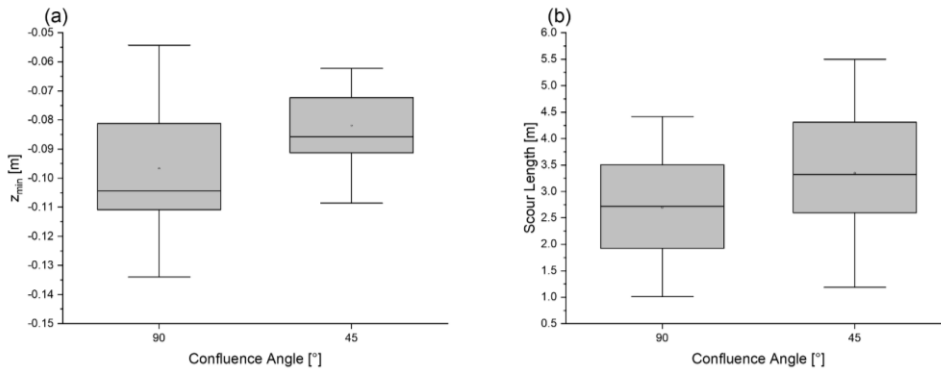
524 and main channel flows, which in turn decreased the turbulence in the confluence producing shallower
525 scour.



526 **Table 7-8** Confluence angle and its impact on the response variables. Post hoc testing was not required
 527 since there are only 2 groups to compare, σ is the standard deviation.

| Response Variable [-] | σ | | Test [-] | Difference in means [-] |
|---------------------------------------|------------|------------|--------------------------------|----------------------------|
| | 45° [-] | 90° [-] | | |
| Z _{max} [m] | 0.02 | 0.02 | T-Test (t statistic = - 0.742) | NO |
| Z _{min} [m] | 0.02 | 0.02 | T Test (t statistic = -2.37) | YES |
| Deposition Area [m ²] | 0.96 | 0.85 | T Test (t statistic = 0.109) | NO |
| Deposition Volume [m ³] | 0.06 | 0.05 | T Test (t statistic = -0.843) | NO |
| Erosion Area [m ²] | 0.98 | 0.87 | T Test (t statistic = -0.199) | NO |
| Erosion Volume [m ³] | 0.03 | 0.03 | T Test (t statistic = -0.425) | NO |
| Deposition Bar Area [m ²] | 0.75 | 0.95 | T Test (t statistic = 1.169) | NO |
| Length Bar [m] | 0.81 | 0.77 | T Test (t statistic = 0.238) | NO |
| Width Bar [m] | 0.10 | 0.10 | T Test (t statistic = 0.916) | NO |
| Scour Area [m ²] | 0.52 | 0.36 | T Test (t statistic = -1.212) | NO |
| Length Scour [m] | 1.22 | 0.88 | T Test (t statistic = -2.04) | YES |
| Width Scour [m] | 0.12 | 0.14 | T Test (t statistic = 1.125) | NO |

528
 529 Additionally, the confluence angle had an impact on the length of the scour (Fig. 12b). Enhanced mixing of
 530 confluent flows, and a reduced hydraulic separation zone created conditions where the scour generally
 531 occupied a greater area but produced a shallower scour depth. However, the width of the bar was relatively
 532 unchanged (Fig. 9e8c) in response to the confluence angle; the increased scour area was represented by
 533 an increase in scour length. While the penetration of the tributary channel was reduced, the transport
 534 capacity of the main channel was still sufficient to mobilize a similar volume of sediment (Fig. 9f8f).



535
 536 **Figure 12** Boxplots from T-Test results for all response variables that showed a significant difference in
 537 mean values (Table 5) with the confluence angle as the controlling factor.

4 Discussion

4—Special dynamics of mountain river confluences

4.1

The confluence angle has been established as one of the main drivers of confluence morphology, thus affecting the ~~and the~~ spatial distribution of the hydraulic zones for lowland confluences. However, for mountain river confluences during events with intense bedload transport it had a minimal effect, corroborating hypothesis 1-, that adjustments to the confluence angle (Fig. 8, Table 8) and the tributary gradient (Fig. 5, Table 5) do not significantly impact confluence morphology and the development of specific geomorphic units. Wohl (2010) discusses the extremal hypotheses (Davies & Sutherland, 1983) which are based on the underlying assumption that the equilibrium channel morphology corresponds to the morphology that maximizes or minimizes the value of a specific parameter (Darby and Van De Wiel, 2003). Examples of this are reductions of unit stream power (Yang & Song, 1979) and energy dissipation rate (Yang, 1976) and maximizations of friction factor (Davies and Sutherland, 1983), and sediment transport rate (White et al., 1982). The confluence morphologically reacted to the steep channel flooding and bedload conditions, characterized by higher velocities, sediment concentrations, and Froude numbers than what would be expected at a lowland confluence, and adjusted to maximize sediment transport through the confluence. Since all channel geometry experiments were exposed to the same discharges and sediment supply rates, a similar development occurred. Lowland regions are typically less intense and morphologically more responsive, relative to mountain river confluences during flooding events, to variations in the size and orientation of the hydraulic zones as they respond to channel adjustments (Mosley, 1976; Best 1987, 1988; Liu et al., 2015). ~~The scour area~~ Scour area and depth were the only response variables sensitive to the confluence angle. Decreasing the confluence angle limited the extent of the flow separation zone (~~compare~~ Mosley, 1976; Best, 1987). The zone of maximum velocity responded ~~sympathetically~~ to the size of the flow separation zone (~~compare~~ Best, 1987). When more channel was available for the zone of maximum velocity from the decreased size of the separation zone, the velocity decreased, causing shallower scour, which is consistent with the findings of Mosley (1976) and Best (1988). In contrast, increasing the confluence angle increased the local velocity and transport capacity and caused greater

Formatted: Heading 2

Formatted: Heading 2, Left

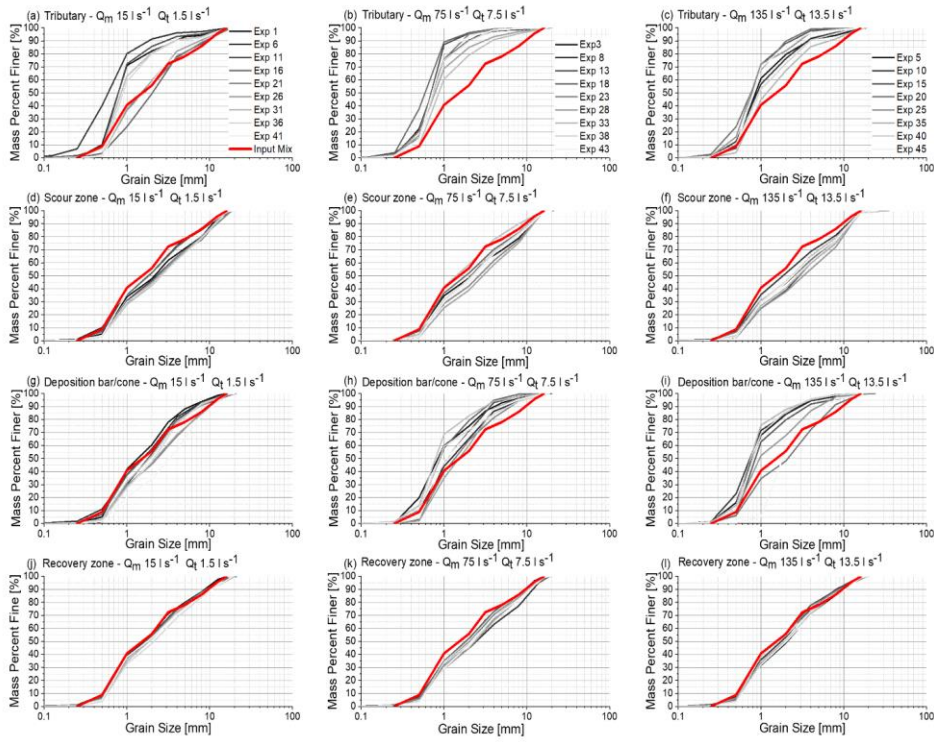
Formatted: Font color: Text 1

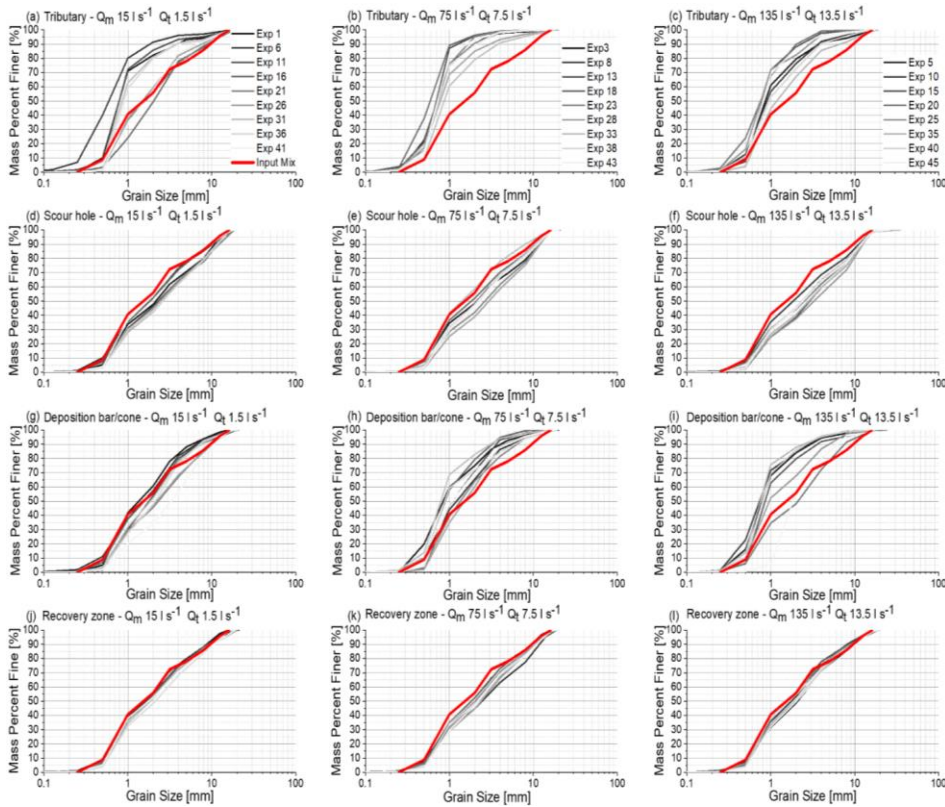
Formatted: Font color: Text 1

566 penetration of the tributary flow. These combined aspects provide evidence that the transport capacity of
567 the main channel is enhanced at higher confluence angles, which was reflected in the tributary depositional
568 volumes and gradients. ~~The tributary channel gradient responding to the transport capacity~~ It has been
569 previously observed in mountain rivers ~~_has been previously observed_~~ (Mueller & Pitlick, 2005; Trevisani et
570 al., 2010) that the tributary channel gradient responds to the transport capacity of the flow. Mueller and
571 Pitlick (2005) suggest that forced changes in gradient are offset by adjustments to width, depth, and bed
572 surface texture to maintain a balance between the intensity and frequency of bed load transport. In confined
573 channels, width adjustments are not possible, resulting in extensive deposition in the channel. The main
574 differences in sediment depositional patterns and mechanisms from adjusting the tributary channel gradient
575 were observed in the tributary channel, while the main channel was largely unchanged. This indicates that
576 with a sustained and abundant sediment supply and relatively uniform main channel hydraulic conditions,
577 the morphologic development of the confluence is not significantly impacted by changes in the tributary
578 channel gradient.

579 Referring to hypothesis 2 ~~(sediment concentration and channel discharge exert the most control over~~
580 depositional and erosional patterns), the same geomorphic units and morphological patterns occurred for
581 all experimental groups and channel configurations, which establishes the dominance of the combined
582 channel discharges over the confluence. This can be explained according to Guillén-Ludeña et al., (2017)
583 where the main channel supplies the dominant flow discharge. The unit stream power in the main channel
584 (Table 4) was sufficient to force the development of the same geomorphic units, for a specific discharge,
585 regardless of changes to sediment concentration and channel geometry. ~~Adjustments to sediment~~
586 concentration were reflected in varying ranges of deposition and erosion depths and volumes, as well as
587 varying extents of these geomorphic units. ~~Adjustments to sediment concentration were shown by a range~~
588 of deposition and erosion depths, volumes, and varying extents of the geomorphic units. Interaction
589 between discharge and sediment shows clear trends of coarsening or fining at specific sites (Fig. 13,
590 Appendix 10) for all the ~~introduced factor~~ introduced controlling factors. However, trends relating sediment
591 concentration or channel geometry to coarsening or fining are not apparent since the same general
592 morphological patterns consistently occurred, which in turn caused similar hydraulic conditions to develop.
593 Grain size distribution curves from the tributary channel near the confluence, the deposition cone or bar,
594 and the recovery zone further illustrate the selective bedload transport occurring in the confluence zone.

595 Consistent across all experiments, the deposited material in the tributary was finer than the input mix (Fig.
596 13a to 13c, Appendix 10). For experiments with the 10-% tributary gradient, this can be explained by the
597 regressive aggradation occurring in the tributary channel, which reduced the gradient of the tributary and,
598 thus, ~~the-its~~ transport capacity. For experiments with a 5-% tributary gradient, the transport capacity of the
599 tributary was saturated, which caused intense progressive deposition of all grain sizes in the channel despite
600 the increased depositional gradient. Samples taken from the scour hole (Fig. 13d to 13f, Appendix 10)
601 showed an overall coarsening, illustrating the enhanced transport capacity through this zone. The
602 separation zone bar was formed in a region of low flow velocity relative to the main channel, which is
603 reflected in the associated grain size distributions (Fig. 13h and 13i, Appendix 10). The samples taken from
604 the lowest discharge experiments were from the deposition cone; the cone did not occupy the hydraulic
605 separation zone and was exposed to the main channel flow. Accordingly, the samples showed a general
606 coarsening pattern of the finer grain fractions and a fining of the larger grain size fractions (Fig. 13g,
607 Appendix 10). The zone of flow recovery is characterized by decreased turbulence and more uniform flow
608 patterns and bed morphology (~~compare~~ Best, 1987; 1988). As a result, no hydraulic or morphologic
609 structures existed that influenced the velocity distribution throughout this portion of the channel. This is
610 apparent in Fig. 13j to 13l where the samples taken across all experiments showed the least deviation from
611 the plotted line of the input material. A slight but overall coarsening is apparent, caused by the increased
612 velocity from the combined channel flow and the resulting selective bedload transport.





614
 615 **Figure 13** Grain size distribution curves from samples taken from the tributary channel (a-c), the scour hole
 616 (d-f), the deposition cone or bar (g-i), and the recovery zone (j-l) for the lowest, middle, and highest
 617 experimental discharges, Q_m and Q_t denote main and tributary channel discharges, respectively.

618
 619 **4.2 Modelling limitations**
 620
 621 Modelling limitations deal mainly with scale effects and the duration required to set up and run an
 622 experiment, limiting the scope of the study, but creating a well-founded base to build from. Preparing and
 623 running an experiment took multiple days; the project duration did not allow investigations into the effects
 624 of the discharge ratio. An ideal experimental program would have included the same 45 experiments but
 625 with a different discharge ratio. Accordingly, we strongly encourage additional investigations into this

626 component as it influences mountain river confluences. All physical models are subject to some degree of
627 scale effects as it is impossible to correctly model all force ratios (Chanson, 2004; Heller, 2011). This arises
628 from having to choose the most relevant force ratio, which for open channel hydraulics is Froude similarity
629 (Heller, 2011). Under Froude similarity, the remaining force ratios cannot be identical between model and
630 prototype and can result in non-negligible scale effects (Heller, 2011). Scale effects generally increase with
631 increasing prototype to model scale factor (Heller, 2011). Scale limitations of grain size diameters are
632 discussed in Zarn (1992), where grain sizes smaller than 0.22 mm can change the flow-grain interaction
633 due to cohesion effects. In this regard, Oliveto and Hager (2005) discuss limiting the D_{50} to 0.80 mm. The
634 model grain size distribution has a minimum grain size of 0.5 mm and a D_{50} of 1.4 mm. The Shields (θ)
635 number and the grain Reynolds (Re^*) number were calculated in the main channel for all discharges and
636 geometric configurations. At the lowest discharge experiments, θ and Re^* at the model scale range from
637 0.08-0.10 and 60-67, respectively. At prototype scale Re^* ranges from 9849-10927. At the next discharge
638 combination, θ and Re^* at the model scale range 0.15-0.17 and 82-87, respectively. At prototype scale Re^*
639 ranges from 13523-14247. While there is certainly a significant shift in Re^* between lab and prototype
640 scales, Aufleger (2006) states that assuming Froude similarity and minimizing scale effects for pre-alpine
641 gravel bed rivers Re^* numbers at the model scale above 80 are recommended. In this regard, for the lowest
642 discharge experiments, the smaller grain fractions were subject to some degree of scale effects.

643 *Formatted: Font: Italic, Font color: Auto*

644 *Formatted: Normal*

646 **5 Conclusion**

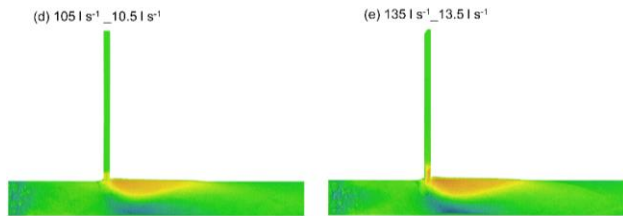
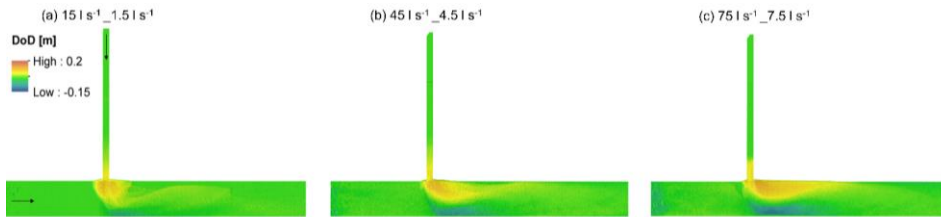
648 The channel discharges and then the tributary sediment concentration are the most impactful factors
649 influencing mountain river confluence morphology during events with intense bedload transport. This
650 conclusion contrasts with the findings of the literature dealing with the controls of river confluences.
651 Mountain river confluences are influenced by characteristics unique to mountain regions, including the
652 availability of massive amounts of sediment and frequent and intense localized flooding. The rate of

653 ~~sediment entering the confluence saturated the transport capacity of the main channel. The resulting~~
654 ~~morphologies represented a system tending towards an equilibrium state, optimized to maximize sediment~~
655 ~~transport through the confluence through local increases in sediment transport rate. Every geometric group~~
656 ~~of experiments had the same discharges and sediment supply rates; the resulting morphologies were similar~~
657 ~~because the channel was responding to similar intense hydraulic and sediment supply conditions. This~~
658 ~~limited the effect the channel adjustments had on the hydraulic zones influencing confluence morphology.~~
659 ~~However, adjustments did cause an apparent response to the depositional mechanisms in the tributary~~
660 ~~channel. A progressive or regressive aggradation of tributary sediment occurred, which enhanced or~~
661 ~~reduced the tributary channel transport capacity. Rapid mutual adjustments occurred as the system tended~~
662 ~~towards an equilibrium state. The evolution towards an equilibrium morphology was characterized by the~~
663 ~~geomorphic units, which reflected the flood magnitude. With increasing discharge, the geomorphic units~~
664 ~~transitioned from a cone to a bank-attached bar as the depositional patterns were forced further downstream~~
665 ~~and into the separation zone, with the bank-attached bar occupying the full extent of the separation zone.~~
666 ~~When sediment concentration was fixed, and the discharge was adjusted, the morphology responded to the~~
667 ~~combined channel flows downstream of the confluence. However, the morphological patterns were mainly~~
668 ~~unaffected when the discharge was fixed and the sediment concentration was adjusted. Therefore, the~~
669 ~~combined discharge determined the overall morphology and the development of specific geomorphic units,~~
670 ~~and the sediment concentration controlled the morphological extent of the units. These aspects illustrate~~
671 ~~that the morphological spatial patterns at mountain river confluences are unique and require special~~
672 ~~attention for flood risk management. The channel discharges and then the tributary sediment concentration~~
673 ~~are the most impactful factors influencing mountain river confluence morphology during events with intense~~
674 ~~bedload transport. This conclusion contrasts with the findings of the a body of literature dealing with the~~
675 ~~controls of river confluences. Mountain river confluences are influenced by characteristics unique to~~
676 ~~mountain regions, including the availability of massive amounts of sediment and frequent localized flooding.~~
677 ~~Because of these combined factors, adjustments to channel geometry did not significantly impact the~~
678 ~~morphological development of the confluence. However, adjustments did cause an apparent response to~~
679 ~~the depositional mechanisms in the tributary channel. A progressive or regressive aggradation of tributary~~
680 ~~sediment occurred, indicating which channel was limiting in terms of transport capacity. Rapid mutual~~
681 ~~adjustments occurred as the channel adjusted to the hydraulic and sediment inputs as the system tended~~

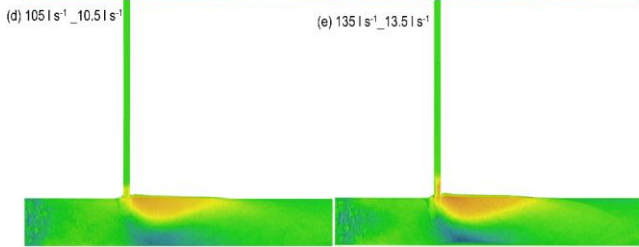
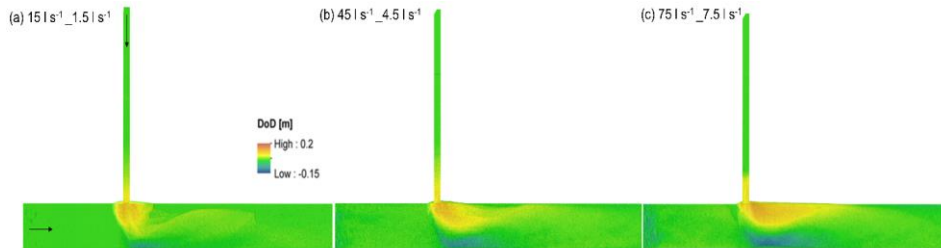
682 towards an equilibrium state. Tending towards an equilibrium morphology was characterized by the
683 geomorphic units, which were indicators of the flood magnitude. When sediment concentration was fixed,
684 and the discharge was adjusted, the morphology responded to the combined channel flows downstream of
685 the confluence. However, the morphological patterns are mainly unaffected when the discharge is fixed and
686 the sediment concentration is adjusted. Therefore, the combined discharge determines the overall
687 morphology and the development of specific geomorphic units, and the sediment concentration controls the
688 morphological extent of the units. These aspects illustrate that the morphological spatial patterns at
689 mountain river confluences are unique and require special attention for flood risk management. Further
690 work should also include assessing ecologically valuable protection measures, including sediment buffer
691 zones.

692 **6 Appendix**

693



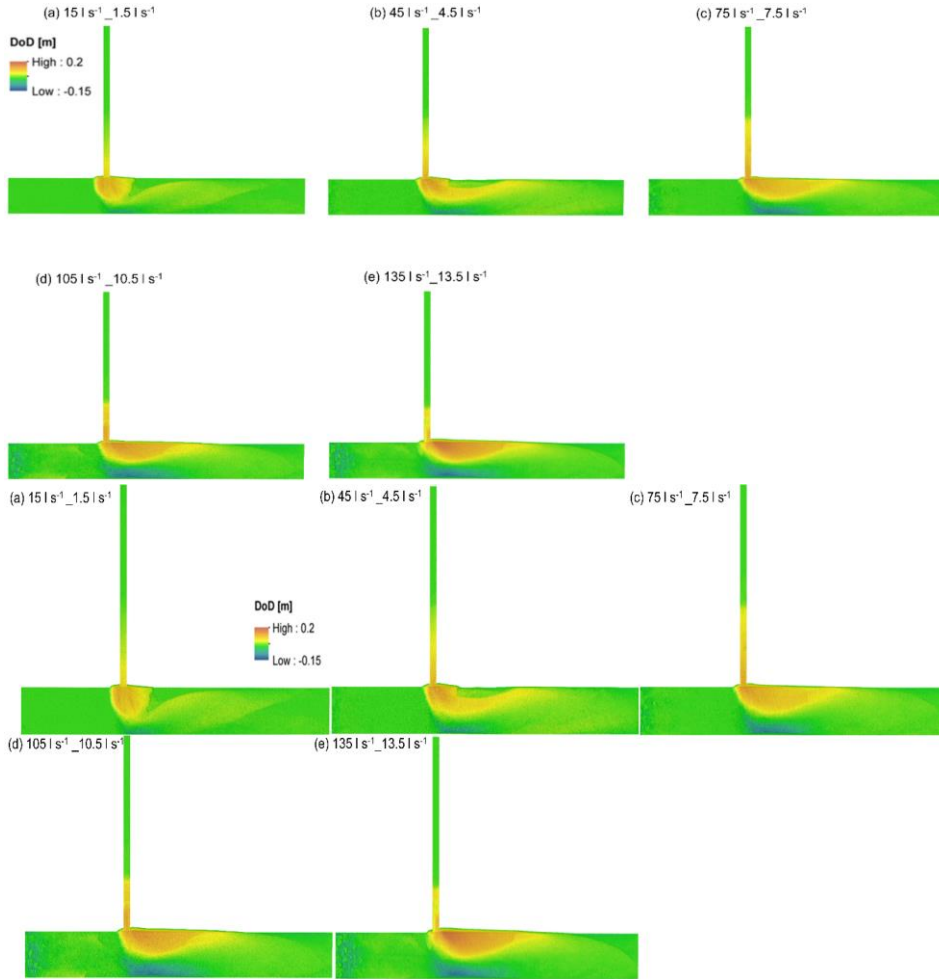
694



695

696 **A 1** Confluence morphology for experiments 1-5 with 5-% sediment concentration, a 90° confluence
 697 angle, and a 10-% tributary gradient.

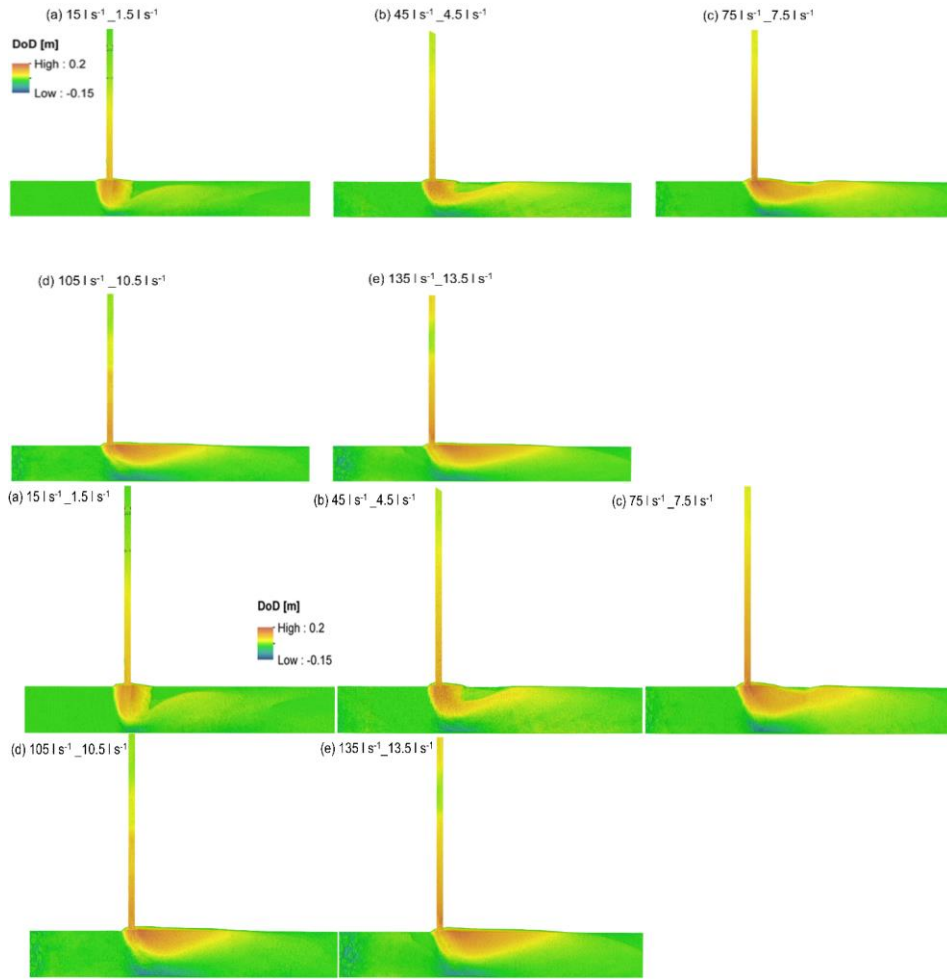
698



699

700

701 **A 2** Confluence morphology for experiments 6-10 with 7.5-% sediment concentration, a 90° confluence
 702 angle, and a 10-% tributary gradient.



703

704

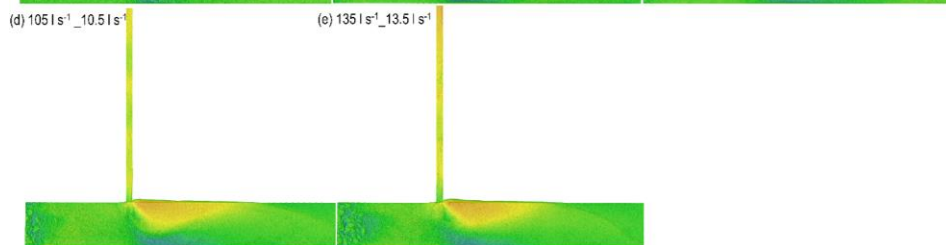
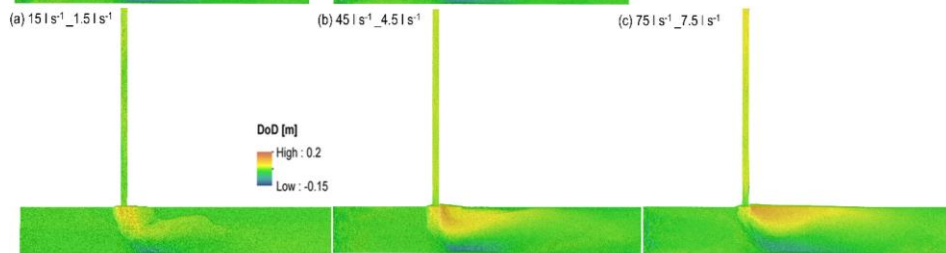
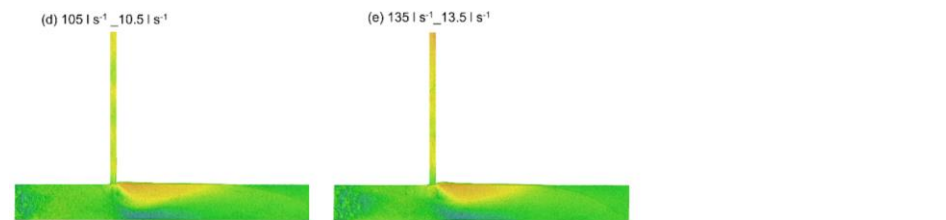
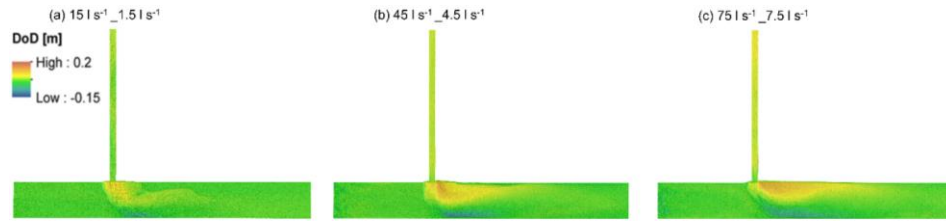
705 **A 3** Confluence morphology for experiments 11-15 with 10% sediment concentration, a 90° confluence

706 angle, and a 10% tributary gradient.

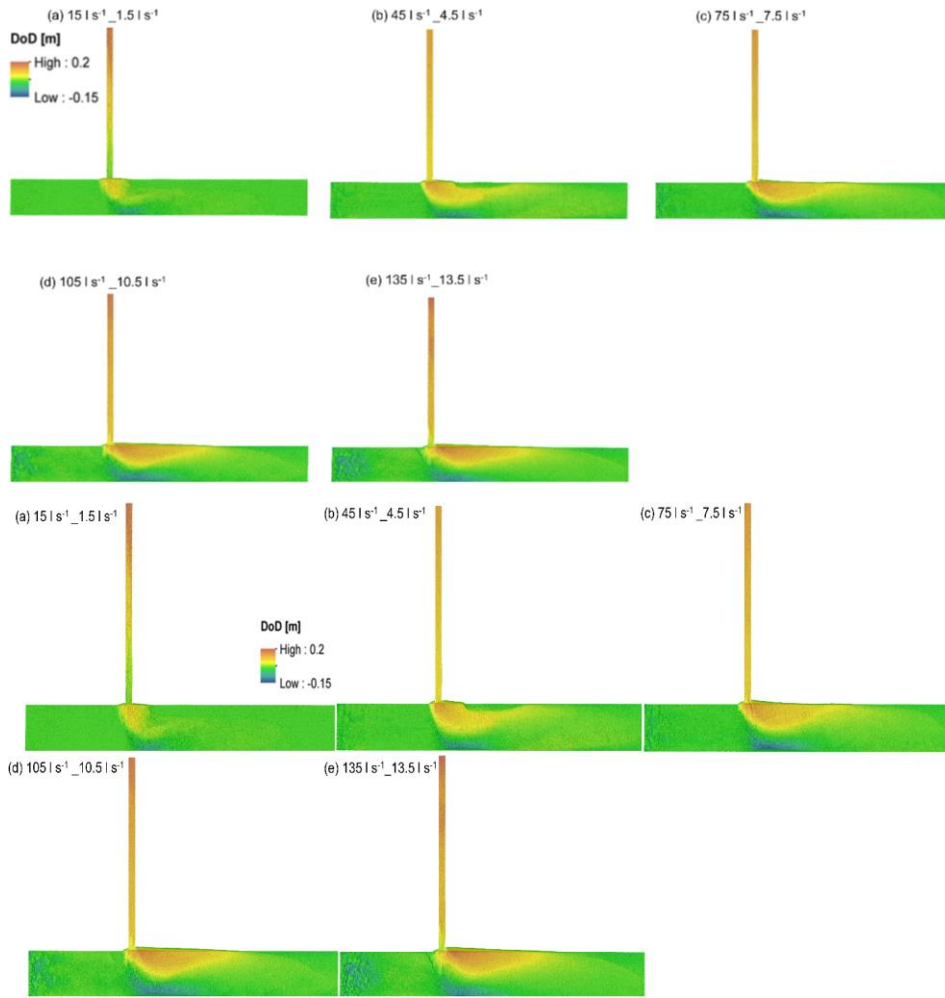
707

Formatted: Font: Not Italic

Formatted: Font: Not Italic



A 4 Confluence morphology for experiments 16-20 with 5-% sediment concentration, a 90° confluence angle, and a 5-% tributary gradient.



712

713

714

715

716

A 5 Confluence morphology for experiments 21-25 with 7.5% sediment concentration, a 90° confluence angle, and a 5% tributary gradient.

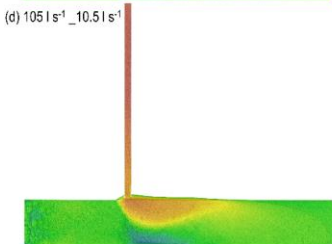
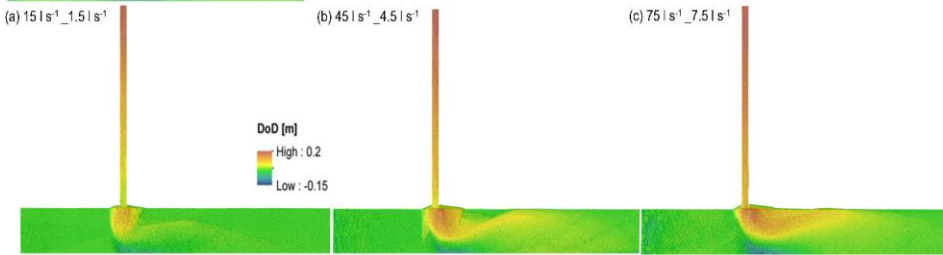
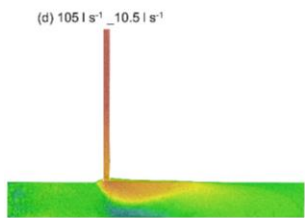
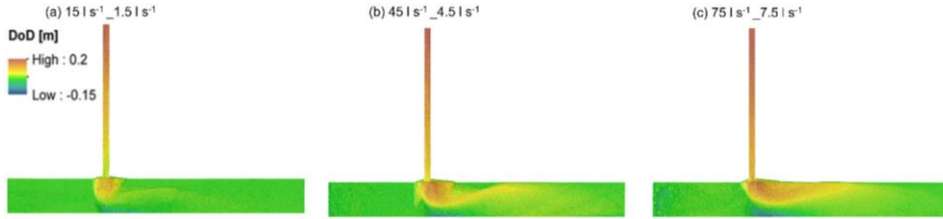
Formatted: Font: Not Italic, Font color: Text 1

Formatted: Font: Not Italic

Formatted: Font: Not Italic

Formatted: Font: Italic, Font color: Auto

Formatted: Normal, Line spacing: single



717

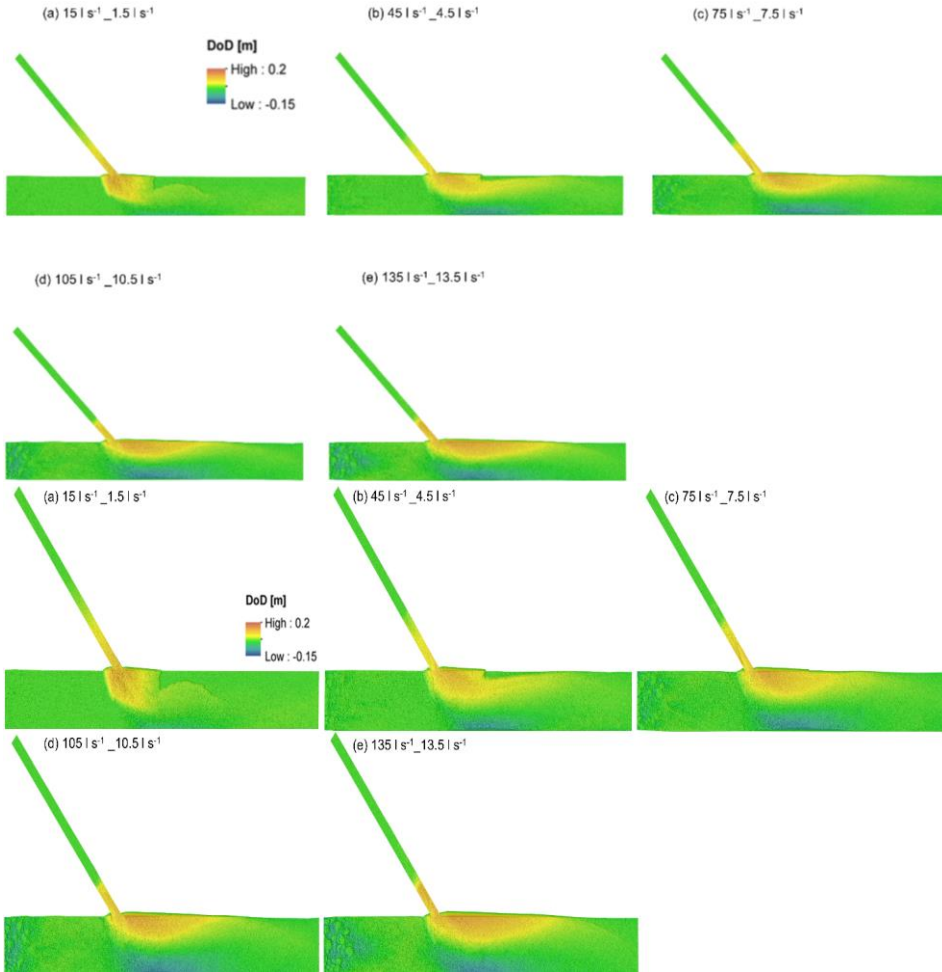
718

719 **A 6** Confluence morphology for experiments 26-29 with 10% sediment concentration, a 90° confluence

720 angle, and a 5% tributary gradient.

Formatted: Font: Not Italic

Formatted: Font: Not Italic



721

722

723 **A 7** Confluence morphology for experiments 31-35 with 5% sediment concentration, a 45° confluence

724 angle, and a 10% tributary gradient.

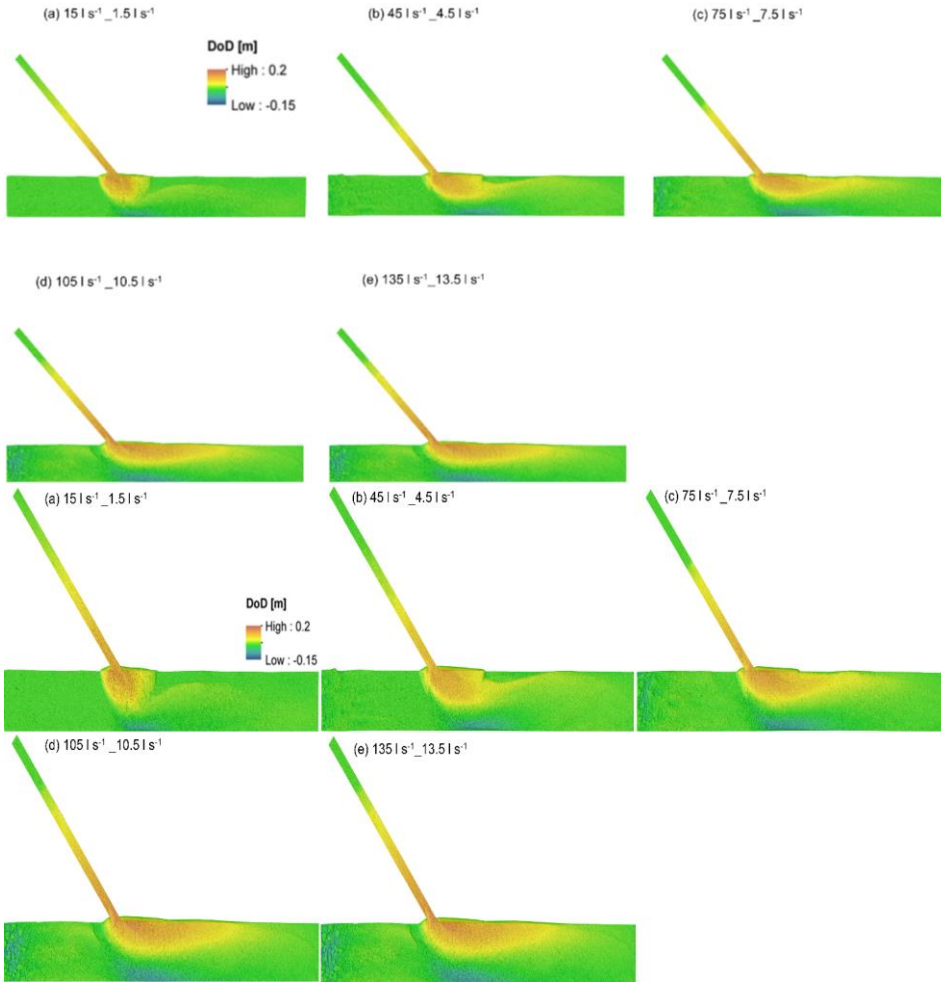
725

Formatted: Font: Not Italic

Formatted: Font: Not Italic

Formatted: Font: Italic

Formatted: Normal, Line spacing: single



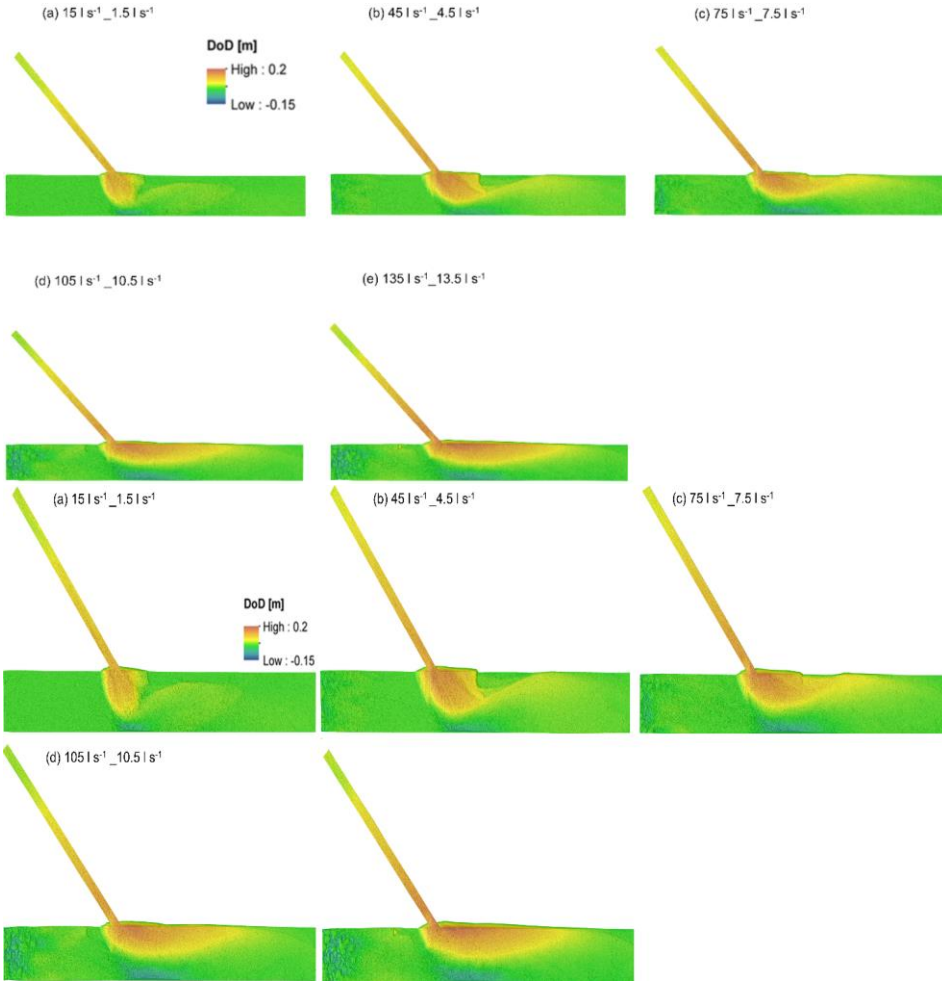
726

727

728 **A 8** Confluence morphology for experiments 36-40 with 7.5-% sediment concentration, a 45° confluence
729 angle, and a 10-% tributary gradient.

730

Formatted: Font: 10 pt, Not Italic, Font color: Text 1
Formatted: Line spacing: Double



731

732

733 **A 9** Confluence morphology for experiments 41-45 with 10% sediment concentration, a 45° confluence
 734 angle, and a 10% tributary gradient.

Formatted: Font: Not Italic

Formatted: Font: Not Italic

735 **A 10** Characteristic grain size for all experiments from samples taken in the tributary channel, the
 736 geomorphic units (~~cone~~, ~~transitional~~, ~~bar~~ depositional, or scour hole), and the recovery zone. Bold text
 737 indicates that the sampled grain size was larger than the input mix grain size.

| Exp | D16 | | | | D50 | | | | D84 | | | | Dm | | | |
|--------------|------------|------------|------------|------------|------------|------------|------------|------------|------------|------------|-------------|-------------|------------|-------------|------------|------------|
| | Trib. | Depo. | Scour | Recov. | Trib. | Depo. | Scour | Recov. | Trib. | Depo. | Scour | Recov. | Trib. | Depo. | Scour | Recov. |
| [-] | [mm] | [mm] | [mm] | [mm] | [mm] | [mm] |
| Input | 0.7 | 0.7 | 0.7 | 0.7 | 1.4 | 1.4 | 1.4 | 1.4 | 6.2 | 6.2 | 6.2 | 6.2 | 2.8 | 2.8 | 2.8 | 2.8 |
| 1 | 0.5 | 0.6 | 0.7 | 0.6 | 0.8 | 1.4 | 2.2 | 1.7 | 2.4 | 4.3 | 9.2 | 6.2 | 1.8 | 2.5 | 4.0 | 3.0 |
| 2 | 0.5 | 0.6 | 0.7 | 0.6 | 0.9 | 1.7 | 2.1 | 1.5 | 2.5 | 5.6 | 9.4 | 6.5 | 1.5 | 2.9 | 4.1 | 3.1 |
| 3 | 0.4 | 0.5 | 0.7 | 0.5 | 0.8 | 0.9 | 2.2 | 1.4 | 1.6 | 2.9 | 9.6 | 6.0 | 1.1 | 1.8 | 4.1 | 2.9 |
| 4 | 0.5 | 0.5 | 0.6 | 0.6 | 0.9 | 0.9 | 1.7 | 1.4 | 3.7 | 2.9 | 8.6 | 6.5 | 2.6 | 1.9 | 3.8 | 3.3 |
| 5 | 0.6 | 0.5 | 0.7 | 0.6 | 0.9 | 0.8 | 2.5 | 1.3 | 2.8 | 2.0 | 10.0 | 6.2 | 2.0 | 1.5 | 4.4 | 3.2 |
| 6 | 0.3 | 0.6 | 0.6 | 0.6 | 0.6 | 1.6 | 1.9 | 1.7 | 1.3 | 4.7 | 7.6 | 6.2 | 1.2 | 2.8 | 3.6 | 3.4 |
| 7 | 0.4 | 0.6 | 0.8 | 0.6 | 0.7 | 1.0 | 3.4 | 1.6 | 0.9 | 3.2 | 12.3 | 6.5 | 0.8 | 2.0 | 5.7 | 3.2 |
| 8 | 0.4 | 0.6 | 0.6 | 0.5 | 0.8 | 1.3 | 2.0 | 1.2 | 1.6 | 3.8 | 9.1 | 6.0 | 1.1 | 2.4 | 4.0 | 3.1 |
| 9 | 0.6 | 0.6 | 0.7 | 0.6 | 0.9 | 0.9 | 2.3 | 1.4 | 1.9 | 3.7 | 7.3 | 6.7 | 1.4 | 2.5 | 3.8 | 3.5 |
| 10 | 0.5 | 0.4 | 0.7 | 0.7 | 0.9 | 0.8 | 1.9 | 1.8 | 3.0 | 2.0 | 9.3 | 6.4 | 1.9 | 1.3 | 4.0 | 2.4 |
| 11 | 0.6 | 0.8 | 0.7 | 0.7 | 0.8 | 1.8 | 2.4 | 2.3 | 1.9 | 5.3 | 10.3 | 9.1 | 1.7 | 3.0 | 4.5 | 4.2 |
| 12 | 0.5 | 0.7 | 0.7 | 0.7 | 0.8 | 1.6 | 2.8 | 3.0 | 2.6 | 3.9 | 11.2 | 11.2 | 1.6 | 2.6 | 5.0 | 3.2 |
| 13 | 0.5 | 0.6 | 0.9 | 0.7 | 0.7 | 1.1 | 5.8 | 1.5 | 1.0 | 3.2 | 13.1 | 7.2 | 0.9 | 1.9 | 6.8 | 3.4 |
| 14 | 0.4 | 0.6 | 0.8 | 0.6 | 0.8 | 1.3 | 5.4 | 1.3 | 1.9 | 3.4 | 13.0 | 4.4 | 1.3 | 2.1 | 6.6 | 2.7 |
| 15 | 0.6 | 0.6 | 0.8 | 0.7 | 0.8 | 0.9 | 3.1 | 1.6 | 1.8 | 2.7 | 11.0 | 6.1 | 1.2 | 1.8 | 5.0 | 3.8 |
| 16 | 0.8 | 0.6 | 0.7 | 0.6 | 2.0 | 1.7 | 1.9 | 1.7 | 6.4 | 5.6 | 3.4 | 6.4 | 3.5 | 3.2 | 3.8 | 3.2 |
| 17 | 0.4 | 0.7 | 0.9 | 0.7 | 0.7 | 1.7 | 4.1 | 1.8 | 0.9 | 5.2 | 3.8 | 6.8 | 0.7 | 2.9 | 5.9 | 3.6 |
| 18 | 0.3 | 0.6 | 0.6 | 0.6 | 0.6 | 0.9 | 1.9 | 1.6 | 1.0 | 2.6 | 3.7 | 6.0 | 0.8 | 1.5 | 3.8 | 3.1 |
| 19 | 0.4 | 0.6 | 0.8 | 0.7 | 0.7 | 1.4 | 3.3 | 1.8 | 1.0 | 5.3 | 3.8 | 7.0 | 0.9 | 2.8 | 5.1 | 3.5 |
| 20 | 0.4 | 0.7 | 0.7 | 0.6 | 0.8 | 2.2 | 2.6 | 1.4 | 1.7 | 6.4 | 3.9 | 6.4 | 1.1 | 3.4 | 4.6 | 3.1 |
| 21 | 0.7 | 0.7 | 0.7 | 0.7 | 1.7 | 2.4 | 2.5 | 2.0 | 6.4 | 7.6 | 3.6 | 7.9 | 3.2 | 3.9 | 4.4 | 3.7 |
| 22 | 0.5 | 0.8 | 0.8 | 0.7 | 0.7 | 1.9 | 3.3 | 1.7 | 1.0 | 4.9 | 4.1 | 6.6 | 0.9 | 3.0 | 5.8 | 3.3 |
| 23 | 0.4 | 0.7 | 0.7 | 0.6 | 0.8 | 1.4 | 2.8 | 1.6 | 1.4 | 4.8 | 3.8 | 7.1 | 1.0 | 2.7 | 4.7 | 3.4 |
| 24 | 0.5 | 0.6 | 0.7 | 0.6 | 0.8 | 1.3 | 2.4 | 1.6 | 1.6 | 4.3 | 3.7 | 6.0 | 1.1 | 2.6 | 4.3 | 3.3 |
| 25 | 0.5 | 0.6 | 0.8 | 0.6 | 0.8 | 1.0 | 3.4 | 1.7 | 2.2 | 3.7 | 3.8 | 6.8 | 1.4 | 2.1 | 5.3 | 3.4 |
| 26 | 0.7 | 0.8 | 0.7 | 0.7 | 1.6 | 2.3 | 2.6 | 2.0 | 5.0 | 7.8 | 3.8 | 7.7 | 2.9 | 4.0 | 4.8 | 3.8 |
| 27 | 0.5 | 0.9 | 0.8 | 0.7 | 0.8 | 2.3 | 3.1 | 1.7 | 1.0 | 5.6 | 3.8 | 6.8 | 0.9 | 3.3 | 5.1 | 3.4 |
| 28 | 0.5 | 0.7 | 0.8 | 0.7 | 0.8 | 1.6 | 3.1 | 1.7 | 1.9 | 3.7 | 3.9 | 7.8 | 1.5 | 2.4 | 5.4 | 3.7 |
| 29 | 0.5 | 0.7 | 0.7 | 0.7 | 0.8 | 1.7 | 2.6 | 1.8 | 1.8 | 5.9 | 3.8 | 6.6 | 1.3 | 3.2 | 4.6 | 3.4 |
| 30 | - | - | - | - | - | - | - | - | - | - | - | - | - | - | - | - |
| 31 | 0.6 | 0.7 | 0.8 | 0.7 | 0.9 | 1.9 | 2.8 | 1.9 | 2.6 | 5.7 | 10.0 | 6.9 | 2.0 | 3.2 | 4.6 | 3.6 |
| 32 | 0.5 | 0.5 | 0.7 | 0.7 | 0.8 | 0.9 | 2.0 | 1.9 | 1.7 | 3.5 | 7.1 | 7.5 | 1.2 | 2.1 | 3.7 | 3.7 |
| 33 | 0.6 | 0.52 | 0.7 | 0.7 | 0.9 | 0.8 | 1.5 | 1.7 | 2.8 | 2.2 | 6.0 | 7.6 | 1.9 | 1.5 | 3.1 | 3.6 |
| 34 | 0.6 | 0.6 | 0.7 | 0.7 | 0.9 | 0.9 | 1.9 | 1.8 | 2.9 | 3.5 | 6.4 | 7.3 | 1.8 | 2.1 | 3.3 | 3.5 |
| 35 | 0.6 | 0.5 | 0.8 | 0.7 | 1.2 | 0.8 | 3.0 | 1.7 | 3.8 | 1.7 | 11.0 | 6.6 | 2.6 | 1.3 | 5.1 | 3.4 |
| 36 | 0.6 | 0.8 | 0.7 | 0.7 | 0.9 | 2.2 | 2.7 | 1.8 | 2.8 | 5.9 | 10.1 | 7.1 | 2.1 | 3.3 | 4.6 | 3.7 |
| 37 | 0.5 | 0.7 | 0.7 | 0.7 | 0.8 | 1.5 | 1.6 | 1.7 | 1.7 | 5.9 | 9.0 | 7.2 | 1.2 | 3.1 | 3.8 | 3.7 |
| 38 | 0.5 | 0.6 | 0.7 | 0.6 | 0.8 | 0.9 | 2.2 | 1.5 | 1.6 | 4.0 | 8.6 | 5.8 | 1.1 | 2.4 | 4.0 | 3.1 |
| 39 | 0.6 | 0.55 | 0.7 | 0.6 | 0.8 | 0.9 | 2.5 | 1.4 | 1.9 | 3.4 | 9.8 | 5.7 | 1.3 | 2.1 | 4.4 | 3.0 |
| 40 | 0.6 | 0.5 | 0.7 | 0.7 | 1.0 | 0.8 | 2.5 | 1.9 | 3.3 | 1.9 | 10.0 | 5.9 | 2.0 | 1.3 | 4.4 | 3.3 |
| 41 | 0.7 | 0.9 | 0.7 | 0.7 | 1.7 | 3.4 | 1.8 | 1.9 | 4.0 | 8.5 | 7.3 | 7.8 | 2.9 | 4.7 | 3.5 | 3.8 |
| 42 | 0.5 | 0.9 | 0.7 | 0.7 | 0.8 | 2.3 | 2.5 | 1.9 | 1.0 | 4.8 | 10.4 | 6.3 | 0.9 | 3.1 | 4.6 | 3.3 |
| 43 | 0.5 | 0.6 | 0.7 | 0.7 | 0.8 | 1.1 | 2.4 | 1.8 | 1.1 | 3.6 | 9.4 | 7.8 | 1.0 | 2.2 | 4.3 | 3.8 |
| 44 | 0.6 | 0.6 | 0.7 | 0.7 | 0.9 | 1.0 | 2.3 | 2.0 | 1.8 | 3.0 | 9.7 | 7.7 | 1.3 | 1.9 | 4.3 | 3.7 |
| 45 | 0.6 | 1.2 | 0.8 | 0.8 | 0.8 | 1.9 | 2.5 | 2.5 | 1.8 | 5.0 | 10.4 | 7.4 | 1.4 | 3.02 | 4.6 | 3.9 |

Formatted Table
 Formatted: Font color: Text 1
 Formatted: Font: Not Bold, Font color: Text 1

738 7 Data Availability

739

740 Data are available from the corresponding author upon reasonable request.

741

742 8 Author Contributions

743

744 TSPO: Conceptualization, data curation, formal analysis, investigation, methodology, visualization, writing
745 – original draft preparation (with input from all co-authors). TK: Formal analysis, data curation. BM:
746 Conceptualization, methodology, writing – review and editing. JH: Formal analysis, investigation, writing –
747 review and editing. AA: Conceptualization, writing – review and editing. FC: Conceptualization, supervision,
748 project administration, funding acquisition, writing – review and editing BG: Conceptualization, supervision,
749 project administration, funding acquisition, writing – review and editing.

750

751 9 Competing Interests

752

753 The authors declare that they have no conflict of interest.

754

755 10 Acknowledgements

756

757 The authors would like to thank the Autonomous Province of Bolzano - South Tyrol – Department of
758 Innovation, Research, University and Museums for funding the project: Towards an Efficient Design of River
759 Confluences to Manage Intense Sediment Impacts from Tributary Torrents (ECOSSED_TT, contract number
760 24/34). This project and the accompanying funding provided the framework to conduct detailed
761 investigations into mountain-river confluence hydraulics and morphology. Additionally, we acknowledge the
762 funding of the Project Anid/Conicyt Fondecyt Regular Folio 1200091 titled “Unravelling the Dynamics and
763 Impacts of Sediment-Laden Flows in Urban Areas in Southern Chile as a Basis for Innovative Adaptation
764 (sedimpact)” led by the PI Bruno Mazzorana.

765 **11** **References**

766 **11**

767 Ancey, C.: Bedload transport: A walk between randomness and determinism. part 1. the state of the art. J.
 768 Hydraul. Res., 58(1), 1–17. doi:10.1080/00221686.2019.1702594, 2020a.

769 Ancey, C.: Bedload transport: A walk between randomness and determinism. part 2. challenges and
 770 prospects. J. Hydraul. Res., 58(1), 18–33. doi:10.1080/00221686.2019.1702595, 2020b.

771 Aulitzky, H.: Preliminary two-fold classification of debris torrents, Conference Proceedings of Interpraevent
 772 1980, Bad Ischl, Austria, 8-12 September, (Vol. 4, 285-309, 1980, translated from German by G.
 773 Eisbacher) Internationale Forschungsgesellschaft, Interpraevent, Klagenfurt. Aufleger, M.:
 774 Flussmorphologische Modell. Grundlagen und Anwendungsgrenzen. Berichte des Lehrstuhls und
 775 der Versuchsanstalt für Wasserbau und Wasserwirtschaft, TU München. Band Nr. 104: 198-207. TU
 776 München, 2006.

777 Aulitzky, H.: Preliminary two-fold classification of debris torrents. Conference Proceedings of Interpraevent
 778 1980, Bad Ischl, Austria, 8-12 September, (Vol. 4, 285-309, 1980, translated from German by G.
 779 Eisbacher.) Internationale Forschungsgesellschaft, Interpraevent, Klagenfurt.

781 Aulitzky, H.: The debris flows of Austria, B. Eng. Geol. Environ., 40, 5-13,
 782 <https://doi.org/10.1007/BF02590338>, 1989.

783 Baranovskiy, N. V.: The development of application to software origin pro for informational analysis and
 784 forecast of forest fire danger caused by thunderstorm activity, J. Automat. Inf. Sci., 51(4), 12-23,
 785 <https://doi.org/10.1615/jautomatinfscien.v51.i4.20>, 2019.

786 Benda, L., Andras, K., Miller, D., and Bigelow, P.: Confluence effects in rivers: Interactions of basin scale,
 787 network geometry, and disturbance regimes, Water Resour. Res., 40(5), 1-15, [https://doi:](https://doi.org/10.1029/2003wr002583)
 788 [10.1029/2003wr002583](https://doi.org/10.1029/2003wr002583), 2004.

789 Best, J. L.: Flow Dynamics at River Channel Confluences: Implications for Sediment Transport and Bed
 790 Morphology, in: Recent Developments in Fluvial Sedimentology, SEPM Special Publication, [edited](#)

- 791 ~~by: edited by:~~ Etheridge, F.G., Flores, R.M. and Harvey, M.D., Society for Sedimentary Geology,
792 Tulsa, OK, 39, 27-35, [https://doi:10.2110/pec.87.39.0027](https://doi.org/10.2110/pec.87.39.0027), 1987.
- 793 Best, J. L.: Sediment transport and bed morphology at river channel confluences, *Sedimentology*, 35, 481-
794 498, [https://doi:10.1111/j.1365-3091.1988.tb00999.x](https://doi.org/10.1111/j.1365-3091.1988.tb00999.x), 1988.
- 795 Biron, P., Roy, A. G., Best, J. L., and Boyer, C. J.: Bed morphology and sedimentology at the confluence
796 of unequal depth channels, *Geomorphology*, 8(2-3), 115-129. [https://doi:10.1016/0169-
797 555x\(93\)90032-w](https://doi.org/10.1016/0169-555x(93)90032-w), 1993.
- 798 [Biron, P., Roy, A. G., & Best, J. L.: Turbulent flow structure at concordant and discordant open-channel
799 confluences. *Exp Fluids*, 21\(6\), 437-446. doi:10.1007/bf00189046, 1996.](#)
- 801 Blöschl, G., Hall, J., Parajka, J., Perdigão, R. A., Merz, B., Arheimer, B., Aronica, G. T., Bilbashi, A.,
802 Bonacci, O., Borga, M., Čanjevac, I., Castellarin, A., Chirico, G. B., Claps, P., Fiala, K., Frolova, N.,
803 Gorbachova, L., Gül, A., Hannaford, J., ... Živković, N.: Changing climate shifts timing of European
804 floods, *Science*, 357(6351), 588-590, [https://doi:10.1126/science.aan2506](https://doi.org/10.1126/science.aan2506), 2017.
- 805 Blöschl, G., Kiss, A., Viglione, A., Barriendos, M., Böhm, O., Brázdil, R., Coeur, D., Demarée, G., Llasat, M.
806 C., Macdonald, N., Retsö, D., Roald, L., Schmocker-Fackel, P., Amorim, I., Bělinová, M., Benito, G.,
807 Bertolin, C., Camuffo, D., Cornel, D., ... Wetter, O.: Current European flood-rich period exceptional
808 compared with past 500 years, *Nature*, 583(7817), 560-566. [https://doi:10.1038/s41586-020-2478-
809 3](https://doi.org/10.1038/s41586-020-2478-3), 2020.
- 810 Boyer, C., Roy, A. G., and Best, J. L.: Dynamics of a river channel confluence with discordant beds: Flow
811 turbulence, bed load sediment transport, and bed morphology, *J. Geophys. Res.*, 111(F4),
812 [https://doi:10.1029/2005jf000458](https://doi.org/10.1029/2005jf000458), 2006.
- 813 Bradbrook, K. F., Biron, P. M., Lane, S. N., Richards, K. S., and Roy, A. G.: Investigation of controls on
814 secondary circulation in a simple confluence geometry using a three-dimensional numerical model,
815 *Hydrological Processes*, 12(8), 1371-1396. [https://doi:10.1002/\(sici\)1099-
816 1085\(19980630\)12:83.0.co;2-c](https://doi.org/10.1002/(sici)1099-1085(19980630)12:8<1371::aid-hydr1099-1085(19980630)12:83.0.co;2-c), 1998.

Formatted: Indent: Left: 0", First line: 0"

- 817 Bunte, K., and Abt, S.R.: Sampling surface and subsurface particle size distributions in wadable gravel-
 818 and cobble-bed streams for analysis in sediment transport, hydraulics, and streambed monitoring,
 819 U.S. Dep. of Agric., For. Serv., Rocky Mt. Res. Stn., Fort Collins, Colorado, USA. Gen. Tech. Rep.
 820 RMRS-GTR-74, 428p, <https://doi.org/10.2737/RMRS-GTR-74>, 2001.
- 821 Chanson, H.: The hydraulics of open channel flow, Butterworth-Heinemann, Oxford, U.K.,
 822 doi:10.1016/B978-0-7506-5978-9.X5000-4, 2004.
- 823 Chow, V.T.: Open Channel Hydraulics, McGraw-Hill, New York, ISBN 9780070859067, 1959.
- 824 Darby, S. E., and M. J. Van De Wiel: Models in fluvial geomorphology, in Tools in Fluvial Geomorphology,
 825 edited by: G. M. Kondolf and H. Piégay, pp. 503–537, John Wiley, Chichester, U.K.,
 826 doi:10.1002/9781118648551.ch17, 2003.
- 827 Davies, T. R. H., and A. J. Sutherland: Extremal hypotheses for river behaviour, Water Resour. Res., 19,
 828 141– 148. doi:10.1029/WR019i001p00141, 1983.
- 829 Delacre, M., Leys, C., Mora, Y., and Lakens, D.: Taking Parametric Assumptions Seriously: Arguments for
 830 the Use of Welch's F-test instead of the Classical F-test in One-Way ANOVA, International Review
 831 Rev. of Soc. Psychology, 32(1), 13, 1-12, <https://doi.org/10.5334/irsp.19>, 2019.
- 832 De Serres, B., Roy, A., Biron, P., and Best, J. L.: Three-dimensional flow structure at a river channel
 833 confluence with discordant beds, *Geomorphology*, 26, 313-335, [https://doi.org/10.1016/S0169-](https://doi.org/10.1016/S0169-555X(98)00064-6)
 834 [555X\(98\)00064-6](https://doi.org/10.1016/S0169-555X(98)00064-6), 1999.
- 835 Dunn, O. J.: Multiple comparisons using rank sums, *Technometrics*, 6(3), 241–252, [https://doi:](https://doi.org/10.1080/00401706.1964.10490181)
 836 [10.1080/00401706.1964.10490181](https://doi.org/10.1080/00401706.1964.10490181), 1964.
- 837 Embleton-Hamann, C.: Geomorphological Hazards in Austria, in: *Geomorphological Hazards of Europe,*
 838 edited by: Embleton, C., and Embleton-Hamann, C., Elsevier Science Amsterdam, NL,
 839 5, 1-30, [https://doi.org/10.1016/S0928-2025\(97\)80002-8](https://doi.org/10.1016/S0928-2025(97)80002-8), 1997.
- 840 Ferguson, R., and Hoey, T.: Effects of Tributaries on Main-Channel Geomorphology, in: *River*
 841 *Confluences, Tributaries and the Fluvial Network*, edited by: Rice, S.P, Roy, A.G. and Rhoads,

Formatted: Font: Not Bold

- 842 B.L., John Wiley & Sons Hoboken, New Jersey, 183-206,
 843 <https://doi.org/10.1002/9780470760383.ch10>, 2008.
- 844 Gems, B., Sturm, M., Vogl, A., Weber, C., and Aufleger, M.: Analysis of Damage Causing Hazard
 845 Processes on a Torrent Fan – Scale Model Tests of the Schnannerbach Torrent Channel and its
 846 Entry to the Receiving Water, Conference Proceedings of Interpraevent 2014 in the Pacific Rim,
 847 Nara, Japan, 25-28 November 2014, 170-178, 2014.
- 848 Gems, B., Kammerlander, J., Aufleger, M., and Moser, M.: Fluviale Feststoffereignisse, in: ExtremA 2019.
 849 Aktueller Wissensstand zu Extremereignissen alpiner Naturgefahren in Österreich, edited by: edited
 850 by: Glade, T., Mergili, M., and Sattler K., Vienna University Press, 287-321, ISBN 9783847110927,
 851 2020.
- 852 Guillén-Ludeña, S., Franca, M. J., Cardoso, A. H., and Schleiss, A.: Hydro-morphodynamic evolution in a
 853 90° movable bed discordant confluence with low discharge ratio, Earth Surf. Processes, 40(14),
 854 1927-1938. <https://doi.org/10.1002/esp.3770>, 2015.
- 855 Guillén-Ludeña, S., Cheng, Z., Constantinescu, G., and Franca, M. J.: Hydrodynamics of mountain-river
 856 confluences and its relationship to sediment transport, J. Geophys. Res.-Earth., 122(4), 901-924.
 857 <https://doi.org/10.1002/2016jf004122>, 2017.
- 858 Hanus, S., Hrachowitz, M., Zekollari, H., Schoups, G., Vizcaino, M., and Kaitna, R.: Future changes in
 859 annual, seasonal and monthly runoff signatures in contrasting Alpine catchments in Austria, Hydrol.
 860 Earth Syst. Sc., 25, 3429-3453. <https://doi.org/10.5194/hess-25-3429-2021>, 2021.
- 861 Heller, V.: Scale effects in physical hydraulic engineering models. J Hydraul Res, 49(3), 293–306.
 862 [doi:10.1080/00221686.2011.578914](https://doi.org/10.1080/00221686.2011.578914), 2011.
- 863 Hübl, J., Ganahl, E., Bacher, M., Chiari, M., Holub, M., Kaitna, R., Prokop, A., Dunwoody, G., Forster, A.,
 864 Schneiderbauer, S.: Dokumentation der Wildbachereignisse vom 22./23. August 2005 in Tirol, Band
 865 1: Generelle Aufnahme (5W-Standard); IAN Report 109 Band 1, Institut für Alpine Naturgefahren,
 866 Universität für Bodenkultur-Wien (unveröffentlicht), 2005.

Formatted: Font: Arial, 10 pt, German (Austria)

Formatted: English (United States)

Formatted: English (United States)

- 867 Hübl, J., and Moser, M.: Risk management in Lattenbach: A case study from Austria, *Wit. Trans. Ecol.*
868 *Envir.*, 90, 333-342, [https://doi:10.2495/deb060321](https://doi.org/10.2495/deb060321), 2006.
- 869 [Hübl J., Eisl J., Tadler R.: Ereignisdokumentation 2012, Jahresrückblick der Ereignisse. IAN Report 150.](#)
870 [Band 3, Institut für Alpine Naturgefahren, Universität für Bodenkultur - Wien \(unveröffentlicht\), 2012.](#)
- 871 ~~Kammerlander, J., Gems, B., Sturm, M., and Aufleger, M.: (2016) Analysis of Flood Related Processes at~~
872 ~~Confluences of Steep Tributary Channels and Their Respective Receiving Streams - 2d Numerical~~
873 ~~Modelling Application, Conference Proceedings of Interpraevent 2016, Lucerne, Switzerland, 30~~
874 ~~May-2 June 2016, 319-326, 2016.~~
- 875 Keiler, M., Knight, J., and Harrison, S.: Climate change and geomorphological hazards in the Eastern
876 European Alps, *Philos. T. R. Soc. A.*, 368(1919), 2461–2479, [https://doi:10.1098/rsta.2010.0047](https://doi.org/10.1098/rsta.2010.0047),
877 2010.
- 878 Knight, J., and Harrison, S.: Sediments and future climate, *Nat. Geosci.*, 2(4), 230–230, [https://doi:](https://doi.org/10.1038/ngeo491)
879 [10.1038/ngeo491](https://doi.org/10.1038/ngeo491), 2009.
- 880 [Lane, E.W.: The importance of fluvial morphology in hydraulic engineering. J. Hydraul. ENG-ASCE. 81, 1–](#)
881 [17, 1955.](#)
- 882 Leite Ribeiro, M., Blanckaert, K., Roy, A. G., and Schleiss, A. J.: Hydromorphological implications of local
883 tributary widening for ~~r~~River ~~r~~Rehabilitation, *Water. Resour. Res.*, 48(10), 201-217, [https://doi:](https://doi.org/10.1029/2011wr011296)
884 [10.1029/2011wr011296](https://doi.org/10.1029/2011wr011296), 2012a.
- 885 Leite Ribeiro, M., Blanckaert, K., Roy, A. G., and Schleiss, A. J.: Flow and sediment dynamics in channel
886 confluences *J. Geophys. Res-Earth.*, 117, F01035-, [https://doi:10.1029/2011jf002171](https://doi.org/10.1029/2011jf002171), 2012b.
- 887 Liu, T., Fan, B., and Lu, J.: Sediment-flow interactions at channel confluences: A flume study, *Adv. Mech.*
888 *Eng.*, 7(6), 1-9, [https://doi:10.1177/1687814015590525](https://doi.org/10.1177/1687814015590525), 2015.
- 889 Löschner, L., Herrnegger, M., Appert, B., Senoner, T., Seher, W., and Nachtnebel, H.P. : Flood risk, climate
890 change and settlement development: a micro-scale assessment of Austrian municipalities. *Reg.*
891 *Environ. Change.* 17, 311–322, [https://doi:10.1007/s10113-016-1009-0](https://doi.org/10.1007/s10113-016-1009-0), 2017.

Formatted: English (United States)

- 892 Massey, F. J.: The Kolmogorov-Smirnov test for goodness of fit, *J. Am. Stat. Assoc.*, 46(253), 68-78,
893 <https://doi.org/10.1080/01621459.1951.10500769>, 1951.
- 894 Maxwell, S. E., and Delaney, H. D.: *Designing experiments and analyzing data* (2nd ed.), ~~Erlbaum,~~
895 ~~MahwahRoutledge,~~ New JerseyYork,
896 <https://doi.org/10.10.4324/97814106092434324/9781315642956>, 2004.
- 897 McKnight, P.E. and Najab, J.: Mann-Whitney U Test. in: *The Corsini Encyclopedia of Psychology* 1-1, John
898 Wiley & Sons, Hoboken, New Jersey, <https://doi.org/10.1002/9780470479216.corpsy0524>, 2010.
- 899 Meunier, M.: *Éléments d'hydraulique Torrentielle*, Cemagref, France, EAN13 9782759212088, 1991.
- 900 Miller, J.P.: High mountain streams: effects of geology on channel characteristics and bed material. *Mem.*
901 *State Bureau of Mines and Mineral Resources, New Mexico Institute of Mining & Technology,*
902 *Socorro, New Mexico* , 4, 1958.
- 903 Moder, K.: Alternatives to F-test in one-way ANOVA in case of heterogeneity of variances (a simulation
904 study). *Psychological Test and Assessment Modeling*, 52(4), 343-353, ISSN 2190-0493, 2010.
- 905 Mosley, M. P.: An experimental study of channel confluences, *J. Geol.*, 84(5), 535-562, [https://doi:](https://doi.org/10.1086/628230)
906 [10.1086/628230](https://doi.org/10.1086/628230), 1976.
- 907 Mueller, E. R., and Pitlick, J.: Morphologically based model of bed load transport capacity in a headwater
908 stream, *J. Geophys. Res.*, 110(F2), [https://doi:10.1029/2003jf000117](https://doi.org/10.1029/2003jf000117), 2005.
- 909 [Oliveto, G., Hager, W.H.: Further results to time dependent local scour at bridge elements. *J. Hydraulic*
910 *Eng.*131\(2\), 97-105, doi:10.1061/\(ASCE\)0733-9429\(2005\)131:2\(97\), 2005.](https://doi.org/10.1061/(ASCE)0733-9429(2005)131:2(97))
- 911 [Penna, N.; De Marchis, M.; Canelas, O.B.; Napoli, E.; Cardoso, A.H.; Gaudio, R.: Effect of the Junction
912 Angle on Turbulent Flow at a Hydraulic Confluence. *Water*, 10, 469, doi:10.3390/w10040469, 2018.](https://doi.org/10.3390/w10040469)
- 913 Prenner, D., Hrachowitz, M., and Kaitna, R.: Trigger characteristics of torrential flows from high to low alpine
914 regions, *Austria, Sci. Total. Environ.*, 658, 958-972, [https://doi:-10.1016/j.scitotenv.2018.12.206,](https://doi.org/10.1016/j.scitotenv.2018.12.206)
915 [20192018.](https://doi.org/10.1016/j.scitotenv.2018.12.206)

- 916 Rhoads, B. and Kenworthy, S.: Flow structure at an asymmetrical confluence.
917 [Geomorphology](https://doi.org/10.1016/0169-555X(94)00069-4), 11, 273-293, [https://doi:10.1016/0169-555X\(94\)00069-4](https://doi.org/10.1016/0169-555X(94)00069-4), 1995.
- 918 Rice, S.: Which tributaries disrupt downstream fining along gravel-bed rivers? *Geomorphology*, 22(1), 39 –
919 56, [https://doi:10.1016/s0169-555x\(97\)00052-4](https://doi.org/10.1016/s0169-555x(97)00052-4), 1998.
- 920 Roca, M., Martín-Vide, J.P., and Martín-Moreta, P.: Modelling a torrential event in a river confluence, *J.*
921 *Hydrol.*, 364, 207-215, [https://doi:10.1016/j.jhydrol.2008.10.020](https://doi.org/10.1016/j.jhydrol.2008.10.020), 2009.
- 922 Rom, J., Haas, F., Hofmeister, F., Fleischer, F., Altmann, M., Pfeiffer, M., Heckmann, T., and Becht, M.:
923 Analysing the large-scale debris flow event in July 2022 in Horlachtal, Austria, using remote sensing
924 and measurement data, *Geosci. J.*, 13(4), 100, [https://doi:10.3390/geosciences13040100](https://doi.org/10.3390/geosciences13040100), 2023.
- 925 Roy, A., and Bergeron, N.: Flow and particle paths at a natural river confluence with coarse bed material,
926 *Geomorphology*, 3(2), 99-112, [https://doi: 10.1016/0169-555x\(90\)90039-s](https://doi.org/10.1016/0169-555x(90)90039-s), 1990.
- 927 [Rudolf-Miklau, F., Suda, J.: Design Criteria for Torrential Barriers, In: Dating Torrential Processes on Fans
928 and Cones. Advances in Global Change Resource, vol 47, edited by: Schnewly-Bollschweiler, M.,
929 Stoffel, M., Rudolf-Miklau, F., Springer, Dordrecht, doi:10.1007/978-94-007-4336-6_26, 2013.](https://doi.org/10.1007/978-94-007-4336-6_26)
- 930 Ruxton, G. D., and Beauchamp, G.: Time for some a priori thinking about post hoc testing, *Behav. Ecol.*,
931 19/3, 690-693, [https://doi:10.1093/beheco/arn020](https://doi.org/10.1093/beheco/arn020), 2008.
- 932 Sawyer, S.: Analysis of Variance: The Fundamental Concepts, *J. Man. Manip. Ther.*, 17, 27E-38E,
933 [https://doi:10.1179/jmt.2009.17.2.27E](https://doi.org/10.1179/jmt.2009.17.2.27E), 2009.
- 934 Steinskog, D. J., Tjøstheim, D. B., and Kvamstø, N. G.: A cautionary note on the use of the Kolmogorov–
935 Simonov test for normality, *Mon. Weather. Rev.*, 135(3), 1151-1157, [https://doi:10.1175/mwr3326.1](https://doi.org/10.1175/mwr3326.1),
936 2007.
- 937 Stevenson, K. J.: Review of OriginPro 8.5, *J. Am. Chem. Soc.*, 133(14), 5621-5621, [https://doi:
938 10.1021/ja202216h](https://doi.org/10.1021/ja202216h), 2011.

- 939 Stoffel, M.: Magnitude–frequency relationships of debris flows — a case study based on field surveys and
 940 tree-ring records, *Geomorphology*, 116(1–2), 67–76, [https://doi:-10.1016/j.geomorph.2009.10.009](https://doi.org/10.1016/j.geomorph.2009.10.009),
 941 2010.
- 942 Stoffel, M., and Huggel, C: Effects of climate change on mass movements in mountain environments, *Prog*
 943 *Phys. Geog.*, 36(3), 421–439, [https://doi:-10.1177/0309133312441010](https://doi.org/10.1177/0309133312441010), 2012.
- 944 St. Pierre Ostrander, T., Holzner, J., Mazzorana, B., Gorfer, M., Andreoli, A., Comiti, F., and Gems, B.:
 945 Confluence morphodynamics in mMountain rRivers in response to intense tributary bedload input,
 946 *Earth Surf. Processes*, 1-22, [https://doi:-10.1002/esp.5613](https://doi.org/10.1002/esp.5613), 2023.
- 947 Sturm, M., Gems, B., Keller, F., Mazzorana, B., Fuchs, S., Papatoma-Köhle, M. and Aufleger, M.:
 948 Experimental analyses of impact forces on buildings exposed to fluvial hazards, *J. Hydrol.*, 565, 1-
 949 13, [https://doi:-10.1016/j.jhydrol.2018.07.070](https://doi.org/10.1016/j.jhydrol.2018.07.070), 2018.
- 950 Trevisani, S., Cavalli, M., and Marchi, L.: Reading the bed morphology of a mountain stream: A
 951 geomorphometric study on high-resolution topographic data, *Hydrol. Earth Syst. Sc.*, 14(2), 393-405,
 952 [https://doi.org:-10.5194/hess-14-393-2010](https://doi.org/10.5194/hess-14-393-2010), 2010.
- 953 Wang, X. K., Wang, X., Lu, W., and Liu, T.: Experimental study on flow behavior at open channel
 954 confluences, *Front. Struct. Civ. Eng.*, 1, 211-216, [https://doi:-10.1007/s11709-007-0025-z](https://doi.org/10.1007/s11709-007-0025-z), 2007.
- 955 Welch, B. L.: The generalization of 'student's' problem when several different population variances are
 956 involved, *Biometrika*, 34 (1–2), 28–35 [https://doi:-10.1093/biomet/34.1-2.28](https://doi.org/10.1093/biomet/34.1-2.28), 1947.
- 957 White, W. R., R. Bettess, and Paris, E.: Analytical approach to river regime, *J. Hydraul. Div. Am. Soc. Civ.*
 958 *Eng.*, 108, 1179– 1193, doi:10.1061/JYCEAJ.0005914, 1982.
- 959 Williams, G. P.; Flume width and water depth effects in sediment-transport experiments, *Sediment transport*
 960 *in alluvial channels, USGS Professional Paper, doi:10.3133/pp562h, 1970.*

Formatted: Font: Arial, 10 pt, Font color: Text 1

Formatted: Font color: Text 1

Formatted: Font: Arial, 10 pt, Font color: Text 1

Formatted: Font color: Text 1

Formatted: Font: Arial, 10 pt, Font color: Text 1

Formatted: Font: Arial, 10 pt, Font color: Text 1

Formatted: Font: Arial, 10 pt, Font color: Text 1

Formatted: Font: Arial, 10 pt, Not Italic, Font color: Text 1

Formatted: Font color: Text 1

Formatted: Font: Arial, 10 pt, Font color: Text 1

Formatted: Default Paragraph Font, Font: (Default) Times New Roman, 12 pt, Font color: Text 1

Formatted: Font: Arial, 10 pt, Font color: Text 1

Formatted: Font color: Text 1

Formatted: Font color: Text 1

- 961 Witte, R. S., & Witte, J. S.: (2017)–Statistics 11th Edition. Wiley and Sons, Hoboken, New Jersey, ISBN
 962 .1119386055, 2017.
- 963 Wohl, E. E.: Mountain rivers revisited. American Geophysical Union/Geopress, Washington, D.C., ISBN
 964 9780875903231, 2010.
- 965 Yang, C. T.: Minimum unit stream power and fluvial hydraulics. J. Hydraul. Div. Am. Soc. Civ. Eng., 102,
 966 919– 934. doi:10.1061/JYCEAJ.0004589. 1976.
- 967 Yang, C. T., and C. C. S. Song: Theory of minimum rate of energy dissipation, J. Hydraul. Div. Am. Soc.
 968 Civ. Eng., 105, 769–784. doi:10.1029/WR017i004p01014, 1979.
- 969 Young, W. J., & Warburton, J.: Principles and practice of hydraulic modelling of braided gravel-bed rivers.
 970 J. Hydrol. (N.Z.), 35(2), 175–198, 1996.
- 971 Zarn, B.: Lokale Gerinneaufweitung: Eine Massnahme zur Sohlenstabilisierung der Emme bei Utzenstorf
 972 (Local river expansion: A measure to stabilize the bed of Emme River at Utzenstorf). VAW Mitteilung
 973 118. D. Vischer ed.ETH Zurich, Zürich [in German], 1992.

Formatted: Font color: Text 1, Not Highlight

Formatted: Font color: Text 1, Not Highlight

Formatted: Justified, Indent: Left: 0", Hanging: 0.44"

Formatted: Font color: Text 1

Formatted: Font color: Text 1

Formatted: Font color: Text 1, Not Highlight

Formatted: Font: 10 pt, Font color: Text 1

Formatted: Font color: Text 1

Formatted: Not Highlight

Formatted: Font: Font color: Custom Color(RGB(34,34,34)), Not Highlight